

AD-783 478

AN ANALYSIS OF MATHEMATICAL TRANS-  
FORMATIONS AND A COMPARISON OF  
NUMERICAL TECHNIQUES FOR COMPUTATION  
OF HIGH-ENERGY CW LASER PROPAGATION  
IN AN INHOMOGENEOUS MEDIUM

Harold J. Breaux

Ballistic Research Laboratories  
Aberdeen Proving Ground, Maryland

June 1974

DISTRIBUTED BY:

**NTIS**

National Technical Information Service  
U. S. DEPARTMENT OF COMMERCE  
5285 Port Royal Road, Springfield Va. 22151

Destroy this report when it is no longer needed.  
Do not return it to the originator.

Secondary distribution of this report by originating  
or sponsoring activity is prohibited.

Additional copies of this report may be obtained  
from the National Technical Information Service,  
U.S. Department of Commerce, Springfield, Virginia  
22151.

ACQUISITION FOR	
ADDS	White Section <input checked="" type="checkbox"/>
	Edm Section <input type="checkbox"/>
ADDS (100)	<input type="checkbox"/>
ADDS (101)	<input type="checkbox"/>
ACQUISITION AVAILABILITY NOTES	
ACQUISITION AVAILABILITY NOTES	
ACQUISITION AVAILABILITY NOTES	

The findings in this report are not to be construed as  
an official Department of the Army position, unless  
so designated by other authorized documents.

2a

UNCLASSIFIED

SECURITY CLASSIFICATION OF THIS PAGE (When Data Entered)

REPORT DOCUMENTATION PAGE		READ INSTRUCTIONS BEFORE COMPLETING FORM
1. REPORT NUMBER REPORT NO. 1723	2. GOVT ACCESSION NO.	3. RECIPIENT'S CATALOG NUMBER <b>AD-783478</b>
4. TITLE (and Subtitle) AN ANALYSIS OF MATHEMATICAL TRANSFORMATIONS AND A COMPARISON OF NUMERICAL TECHNIQUES FOR COMPUTATION OF HIGH-ENERGY CW LASER PROPAGATION IN AN INHOMOGENEOUS MEDIUM		5. TYPE OF REPORT & PERIOD COVERED Final
		6. PERFORMING ORG. REPORT NUMBER
7. AUTHOR(s) Harold J. Breaux		8. CONTRACT OR GRANT NUMBER(s)
9. PERFORMING ORGANIZATION NAME AND ADDRESS USA Ballistic Research Laboratories Aberdeen Proving Ground, Maryland 21005		10. PROGRAM ELEMENT, PROJECT, TASK AREA & WORK UNIT NUMBERS RDT&E 1T662609A308
11. CONTROLLING OFFICE NAME AND ADDRESS US Army Materiel Command 5001 Eisenhower Avenue Alexandria, Virginia 22333		12. REPORT DATE JUNE 1974
		13. NUMBER OF PAGES 49
14. MONITORING AGENCY NAME & ADDRESS (if different from Controlling Office)		15. SECURITY CLASS. (of this report)  UNCLASSIFIED
		15a. DECLASSIFICATION/DOWNGRADING SCHEDULE
16. DISTRIBUTION STATEMENT (of this Report)  Approved for public release; distribution unlimited.		
17. DISTRIBUTION STATEMENT (of the abstract entered in Block 20, if different from Report)		
18. SUPPLEMENTARY NOTES		
19. KEY WORDS (Continue on reverse side if necessary and identify by block number)  Thermal Blooming                      Thermal Lens Nonlinear Propagation Nonlinear Optics Laser Beams		
20. ABSTRACT (Continue on reverse side if necessary and identify by block number) emj  Present methods for modeling the propagation of focused and collimated laser beams are examined. Methods used for transforming the paraxial equation into a form more suitable for computation are generalized. This generalization is shown to lead to more beneficial computational characteristics than transformations previously employed. Various strategies arising from these transformations are analyzed and compared for numerical efficiency. The transformed equations are shown to be a convenient point of departure for solution by a		

20. Abstract (Cont.)

class of numerical methods. The formulation is shown to lead to a Fast Fourier Transform (FFT) solution that does not require a Nyquist accuracy criterion, allowing the numerical procedure to march the solution forward in a more economical fashion. Typical propagation problems are solved by this method and compared with the numerical solution and computational cost obtained by use of an Implicit-Galerkin-Spline technique now in common use. The FFT solution technique is found to be the more efficient and easiest to implement in computer codes.

2

UNCLASSIFIED

## TABLE OF CONTENTS

	<u>Page</u>
LIST OF FIGURES . . . . .	5
I. INTRODUCTION . . . . .	7
II. MATHEMATICAL MODEL . . . . .	8
III. TRANSFORMATIONS . . . . .	9
IV. IMPLICIT-GALERKIN-SPLINE METHOD . . . . .	12
V. FAST FOURIER TRANSFORM METHOD . . . . .	15
VI. PHASE INITIALIZATION . . . . .	18
VII. CHOICE OF SCALING LENGTH FOR ADAPTIVE COORDINATES . . . . .	19
VIII. A COMPARISON OF THE ACCURACY AND EFFICIENCY OF THE TWO METHODS . . . . .	22
IX. CONCLUSIONS . . . . .	40
ACKNOWLEDGMENTS . . . . .	40
REFERENCES . . . . .	41
APPENDIX A - USE OF FAST FOURIER TRANSFORM SUBROUTINES . . . . .	45
APPENDIX B	
I. Listing of FORTRAN IV Subroutine for One Step IGS Advance . . . . .	47
II. Listing of FORTRAN IV Subroutine for One Step FFT Advance . . . . .	49
LIST OF SYMBOLS . . . . .	51
DISTRIBUTION LIST . . . . .	53

## LIST OF FIGURES

<u>Figure</u>	<u>Page</u>
1. Problem 1 - Effect of Changing $\Delta z$ for IGS Method . . . . .	24
2. Problem 1 - Effect of Changing $\Delta z$ for IGS Method . . . . .	25
3. Problem 1 - Effect of Changing $\Delta z$ for FFT Method . . . . .	26
4. Problem 1 - Effect of Changing $\Delta z$ for FFT Method . . . . .	27
5. Aperture Plane Contours - Same for All Nine Cases . . . . .	30
6. IGS Method - Grid Too Coarse - Phase Oscillations Not Removed . . . . .	31
7. IGS Method - Phase Oscillations Not Removed . . . . .	32
8. IGS Method - IGS Method - x,y Grid Too Coarse . . . . .	33
9. IGS Method - Phase Oscillations Removed - Finer Gridding .	34
10. IGS Method - Nyquist Criterion Ignored, $\Delta z$ Too Large . . .	35
11. IGS Method - Nyquist Criterion Ignored, $\Delta z$ Too Large . . .	36
12. FFT Method - Phase Oscillations Not Removed . . . . .	37
13. FFT Method - Excellent Solution with Coarser x,y Grid and No Nyquist Criterion (10 z Steps) . . . . .	38
14. FFT Method - Acceptable Solution with Coarser x,y Grid and No Nyquist Criterion (5 z Steps) . . . . .	39

### Table

1. Summary of Key Parameters for Problem 2 . . . . .	29
--	----

## I. INTRODUCTION

A problem of considerable current interest is the modeling of laser propagation through inhomogeneous media. Of particular interest is the case where the index-of-refraction inhomogeneities are induced by high-energy beams interacting with the medium. The self-consistent modeling of the problem requires the modeling of the hydrodynamics of this interaction, the effect of the hydrodynamics on the index field, and the influence of this induced field on the propagation. Such models have been derived from first principles by a number of authors.<sup>1-6\*</sup> The effect of the phenomenon has been examined by use of analytical approximations<sup>7,8</sup> and by numerical solution employing a number of algorithms.<sup>1-21\*\*</sup> The most successful algorithm now used by several of the large-scale computer codes is the so-called Implicit-Galerkin-Spline (IGS) technique devised by Herrman and Bradley.<sup>9</sup> Even more important than the numerical algorithm, however, is the form in which the model is preprocessed for computation. Experience indicates that focused beams of high Fresnel number require the model's being specified in an adaptive coordinate system; otherwise, as the marching computations approach the focus, spatial resolution is insufficient for any numerical scheme utilizing a reasonable number of grid points. Furthermore, the focusing (defocusing) strategy must allow for the fact that the beam will be distorted and spread to an extent usually lying somewhere in expanse between the exit-plane spot size and the so-called diffraction-limited spot size at the focus. For high Fresnel numbers the transformations to adaptive coordinates must be accompanied by an appropriate phase transformation; otherwise, phase oscillations cannot be sampled adequately. Transformations previously used to overcome this difficulty either partially removed the initial phase oscillation and allowed arbitrary coordinate focus (defocus)<sup>2,3,5</sup> or removed all the initial phase but were limited to a focusing strategy following the behavior of a beam focused in vacuum.<sup>9,10\*</sup>

The generalized transformations derived herein contain the best features of both these cited methods and are shown to be a convenient point of departure for solution by a class of numerical methods. Two computer codes utilizing these transformations have been developed and compared, one using a modified form of the Herrmann-Bradley algorithm and the other using a Fast Fourier Transform (FFT) approach described herein. The formulation cited above is shown to lead to an FFT solution that does not require a Nyquist accuracy criterion, allowing the numerical procedure to march the solution forward in a more economical fashion. Numerical experiments indicate that the IGS method is slightly faster on a per step basis when identical grid spacing is used. The FFT approach, however, yields greater accuracy for identical spacing of mesh in the

---

\*References are listed on page 41.

\*\*This list is representative but by no means complete.

\*\*\*See note after Reference 9.

transverse plane and, because of larger allowable propagation steps, it is overall faster. This factor, in conjunction with the greater ease of implementing an FFT algorithm, and the requirement for less core storage (when symmetry is not assumed), makes the method superior to algorithms currently used.

The algorithms described herein concern themselves primarily with the solution of the propagation equation. The class of problems addressed is represented by hydrodynamic equations which can be solved essentially in closed form within each computing step. This is the type of problem to which most attention has been directed in the literature.

Stimulus for the FFT portion of this report arose from a three-way consultation between the author, Dr. J. Wallace of Far Field, Inc., Sudbury, Massachusetts, and Dr. J. Lilly of the US Army Missile Command. A related FFT technique for the wave equation and hydrodynamics for repetitively pulsed lasers is described in an Army Missile Command Report<sup>22</sup> which is in preparation. The nature of this collaboration is described in Section V and the Acknowledgment.

## II. MATHEMATICAL MODEL

We consider the model applicable to continuous-wave operation of a laser in steady-state conditions. We assume that the laser is propagating through an atmosphere with a time-independent cross wind  $V(\xi)$  and is being rotated (slewed) at an angular rate  $\Omega$  through an axis passing through the exit aperture. We assume that the hydrodynamics can be represented by the steady-state heat equation with the laser acting as a source term, that the wind and slewing produce forced convection, and that conductivity is negligible. Under these assumptions the governing model is given by<sup>1</sup>

$$2ik \frac{\partial W}{\partial \zeta} + (\frac{\partial^2 W}{\partial \xi^2} + \frac{\partial^2 W}{\partial n^2}) + k^2(n^2 - n_0^2)W = 0, \quad (2-1)$$

$$n^2 - n_0^2 = (n_0^2 - 1)\Delta\rho/\rho = -(n_0^2 - 1)\Delta T/T_0, \quad (2-2)$$

$$\rho_0 c_p (V + \Omega \zeta) \frac{\partial (\Delta T)}{\partial \xi} = \alpha_1 e^{-\alpha_1 \xi} |W|^2, \quad (2-3)$$

$$W(\xi, n, 0) = (P/\pi r^2) F(\xi, n) \exp[i\phi - i(k/R)(\xi^2 + n^2)/2]. \quad (2-4)$$

Equation (2-1) is the paraxial approximation to the wave equation. Equation (2-2) is obtained from the Lorentz-Lorenz law expressing the change in the index of refraction as a function of the change in temperature or air density where small deviations from ambient are assumed. Equation (2-3) is the expression of the heat balance for the conditions



stated above. Equation (2-4) expresses the amplitude and phase of the launched beam. In (2-4) the two quantities in the complex exponential represent the phase arising from the laser cavity and the focusing optics, respectively. It should be noted that in Equation (2-3) we have neglected the so-called kinetic cooling phenomenon,<sup>2,3</sup> since this effect is insignificant for ground-based lasers. This effect can nevertheless be brought into this model without change in the basic nature of the algorithm, since it merely affects a quadrature formula.<sup>1,3,5</sup>

We convert the model to a form containing all variables in dimensionless form by letting

$$U = W/(P/\pi r^2)^{1/2}, \quad (2-5)$$

$$X = \xi/r, \quad Y = \eta/r, \quad (2-6)$$

$$Z = \zeta/L, \quad (2-7)$$

$$\alpha = \alpha_0 L, \quad (2-8)$$

$$\beta = kr^2/L, \quad (2-9)$$

$$\gamma = (n_0^2 - 1) P / (T_0 \rho_0 c_p V \lambda r), \quad (2-10)$$

$$\mu = \frac{1}{2} kL(n^2 - n_0^2), \quad (2-11)$$

$$\omega = \Omega L/V, \quad (2-12)$$

$$f(X,Y) = F(Xr,Yr), \quad (2-13)$$

$$\phi(X,Y) = \Phi(Xr,Yr). \quad (2-14)$$

Here we have assumed that  $r$  is a convenient scale length in the transverse  $(\xi, \eta)$  plane. For a gaussian beam a convenient choice for  $r$  is the  $e^{-1}$  folding radius. For focused beams the characteristic length,  $L$ , in the  $\zeta$  direction, is conveniently chosen to be the focal distance  $R$ . In order to make one set of equations valid for focused beams and collimated beams ( $R=\infty$ ),  $L$  is defined by

$$L = \begin{cases} R, & \text{focused beams} \\ kr^2, & \text{collimated beams.} \end{cases} \quad (2-15)$$

For this choice of dimensionless variables the model takes the form

$$2i\beta\partial U/\partial Z + (\partial^2 U/\partial X^2 + \partial^2 U/\partial Y^2) + 2\beta\mu U = 0, \quad (2-16)$$

$$\mu(X,Y,Z) = -\alpha\gamma e^{-\alpha Z} (1 + \omega Z)^{-1} \int_{-\infty}^X |U(X',Y,Z)|^2 dx', \quad (2-17)$$

$$U(X,Y,0) = f(X,Y) \exp[i\phi - i\beta_1(X^2 + Y^2)/2], \quad (2-18)$$

where

$$\beta = \begin{cases} kr^2/R, & \text{focused beams} \\ 1, & \text{collimated beams,} \end{cases} \quad (2-19)$$

and

$$\beta_1 = \begin{cases} \beta, & \text{focused beams} \\ 0, & \text{collimated beams.} \end{cases} \quad (2-20)$$

The solution to the model expresses the dimensionless irradiance  $|U|^2$  as a function of the four dimensionless parameters  $\alpha, \beta, \gamma, \omega$  and  $X, Y, Z$ . If we seek the maximum irradiance or a characteristic average irradiance in the focal plane, then the solution is seen to be dependent only on  $\alpha, \beta, \gamma$  and  $\omega$ .

Equation (2-16) is of parabolic type, and the algorithms successfully utilized for solution have similarities to those employed for numerical solution of the time-dependent heat equation. The  $Z$  variable, representing the propagation direction, is analogous to the time variable in heat transfer. The various methods used thus far "march" the computations forward in  $Z$  as is done in the classical explicit and implicit difference schemes. Equation (2-18) is used for specifying the initial plane of data. At each step the index distribution is recalculated, utilizing the most current values for  $U$  where  $\Delta T$ , as will be shown, is evaluated by numerical quadrature. Despite these similarities to the heat transfer problem, the algorithms referenced above have, of necessity, been uniquely tailored to the propagation problem and are somewhat more complicated than the techniques used for solving the classical heat equation. Factors of computing efficiency of 10-100 can be gained by transforming the above model into a form more suitable for computation. These transformations are essential regardless of the numerical algorithm ultimately used.

### III. TRANSFORMATIONS

Adaptive coordinates are generally required for focused beams of high Fresnel number but have also been found necessary for collimated beams when significant beam spreading occurs. The transformations utilized for adaptive coordinates and phase removal are as follows:

$$x = X/a(Z), \quad y = Y/a(Z), \quad (3-1)$$

$$U = [B/a(Z)] \exp\left[\frac{1}{2} i\beta (X^2 + Y^2) (\partial a / \partial Z) / a(Z)\right], \quad (3-2)$$

$$z = \int_{z_0}^Z (\beta a^2)^{-1} dz. \quad (3-3)$$

The application of these transformations to (2-16) results in

$$2i \partial B / \partial z + (\partial^2 B / \partial x^2 + \partial^2 B / \partial y^2) + g(x, y, Z) B = 0 \quad (3-4)$$

where

$$g(x, y, Z) = 2\beta a^2 \mu - \beta^2 (x^2 + y^2) a^3 \partial^2 a / \partial Z^2. \quad (3-5)$$

The choice of the term  $(\partial a / \partial Z) / a$  in the phase transformation (3-2) makes possible the maintenance of a simple structure for the transformed propagation equation for any subsequent choice of scale length  $a(Z)$ . All first-order derivatives  $B_x, B_y$  that would otherwise appear in the transformed equation have been eliminated by this particular choice of variables. The transformations (3-1), (3-2), and (3-3) are a generalization of transformations used by Wallace,<sup>2</sup> Aitken et al.,<sup>3</sup> and Herrmann and Bradley.<sup>9</sup> By appropriate choice of  $a$ , these cited transformations result from the above generalization. In a later section we will show how certain advantages peculiar to each of the cited system of transformations can be obtained by appropriate choice of  $a(Z)$ .

The solution to (3-4) is highly oscillatory in  $z$ , portending difficulty in numerical computation due to the Nyquist criterion. The oscillations arising from the term containing  $g$  are removed by use of the Herrmann-Bradley<sup>9</sup> transformation

$$D = B \exp(-i\Gamma/2) \quad (3-6)$$

where

$$\Gamma = \int_{z_0}^z g(x, y, Z) dz. \quad (3-7)$$

This leads to the equation

$$2i \partial D / \partial z = -\exp(-\frac{1}{2} i\Gamma) (\partial^2 / \partial x^2 + \partial^2 / \partial y^2) [D \exp(-\frac{1}{2} i\Gamma)]. \quad (3-8)$$

If we envision the approximation of (3-8) by finite differences, where all difference operators are centered at  $z = z_0 = z_n + \Delta z_n / 2$ , then all terms containing  $\Gamma$  become unity. The resulting difference equation is then identical to the difference equation arising for a collimated beam in vacuum. The difference approximation to Equation (3-8) is then indistinguishable from the approximation to

$$2i \partial D / \partial z = -(\partial^2 / \partial x^2 + \partial^2 / \partial y^2) D. \quad (3-9)$$

In sequence with the transformations leading to it, Equation (3-9) is the point of departure for numerical solution using both the IGS and FFT methods.

#### IV. IMPLICIT-GALERKIN-SPLINE METHOD

The IGS algorithm is designed to advance the solution of Equation (3-9) from the plane  $z_n$  to the plane  $z_{n+1} = z_n + \Delta z$ . The algorithm, in conjunction with the initial wave function specification, is applied repetitively, along with phase initializations at each step, to march the solution to the point in  $z$  of interest. Since we have assumed the wind to be along the  $x$ -axis, we have a line of symmetry along  $y=0$ . We use this symmetry to reduce the calculations in half. In the rectangular propagating tube

$$\begin{aligned} -X_M &\leq x \leq X_M, \\ 0 &\leq y \leq Y_M, \\ 0 &\leq z \leq z_M, \end{aligned} \tag{4-1}$$

we superimpose the three-dimensional grid

$$\begin{aligned} x_j &= -X_M + (j-1)\Delta x, \quad j = 1, 2, \dots, J \\ y_k &= (k-1)\Delta y, \quad k = 1, 2, \dots, K \\ z_{n+1} &= z_n + \Delta z_n, \quad n = 1, 2, \dots, M. \end{aligned} \tag{4-2}$$

On this grid we approximate Equation (3-9) by a Crank-Nicholson type stencil in  $z$  and the resulting difference equation by a fractional step-alternating direction approximation. This leads to the two equations:

$$\left(1 - \frac{1}{4} i\Delta z \partial^2 / \partial x^2\right) D^{n+\frac{1}{2}} = \left(1 + \frac{1}{4} i\Delta z \partial^2 / \partial x^2\right) D^n, \tag{4-3}$$

$$\left(1 - \frac{1}{4} i\Delta z \partial^2 / \partial y^2\right) D^{n+1} = \left(1 + \frac{1}{4} i\Delta z \partial^2 / \partial y^2\right) D^{n+\frac{1}{2}}, \tag{4-4}$$

where the superscripts denote the wave function at the  $n$ ,  $n+\frac{1}{2}$ , and  $n+1$   $z$  levels, respectively.

The linear spline approximation<sup>9</sup> is given by

$$D \approx \bar{D} = \sum_{\ell=1}^J \sum_{m=1}^K D_{\ell,m} \omega_{\ell}(x) \omega_m(y) \tag{4-5}$$

where

$$\omega_\ell(x) = \begin{cases} 0, & x \leq x_{\ell-1} \text{ or } x \geq x_{\ell+1}, \quad \ell \neq 1, J \\ (x - x_{\ell-1})(x_\ell - x_{\ell-1})^{-1}, & x_{\ell-1} \leq x \leq x_\ell, \quad \ell \neq 1, J \\ (x_{\ell+1} - x)(x_{\ell+1} - x_\ell)^{-1}, & x_\ell \leq x \leq x_{\ell+1}, \quad \ell \neq 1, J \end{cases} \quad (4-6)$$

$$\omega_1(x) = \exp \frac{1}{2} (x_1^2 - x^2), \quad -\infty \leq x \leq x_1 \quad (4-7)$$

$$\omega_J(x) = \exp \frac{1}{2} (x_J^2 - x^2), \quad x_J \leq x \leq \infty. \quad (4-8)$$

A similar definition applies to  $\omega_m(y)$ .

Applying the Galerkin method<sup>24</sup> to (4-3), one obtains

$$\int_{-\infty}^{\infty} \omega_j(x) \left[ \left(1 - \frac{1}{4} i \Delta z \partial^2 / \partial x^2\right) \bar{D}^{n+\frac{1}{2}} - \left(1 + \frac{1}{4} i \Delta z \partial^2 / \partial x^2\right) \bar{D}^n \right] dx = 0, \quad (4-9)$$

with a similar expression resulting from (4-4). After performing the integration, one obtains two sets of coupled linear equations given by

$$\begin{aligned} & (1 - ia_1)(D_{j-1,k}^{n+\frac{1}{2}} + D_{j+1,k}^{n+\frac{1}{2}}) + (4 + 2ia_1)D_{j,k}^{n+\frac{1}{2}} \\ & = (1 + ia_1)(D_{j-1,k}^n + D_{j+1,k}^n) + (4 - 2ia_1)D_{j,k}^n, \end{aligned} \quad (4-10)$$

$$\begin{aligned} & (1 - ia_1)(D_{j,k-1}^{n+1} + D_{j,k+1}^{n+1}) + (4 + 2ia_1)D_{j,k}^{n+1} \\ & = (1 + ia_1)(D_{j,k-1}^{n+\frac{1}{2}} + D_{j,k+1}^{n+\frac{1}{2}}) + (4 - 2ia_1)D_{j,k}^{n+\frac{1}{2}}, \end{aligned} \quad (4-11)$$

where

$$a_1 = 3/2 \Delta z / h^2, \quad (4-12)$$

$$h = \Delta x = \Delta y. \quad (4-13)$$

It should be noted that the effect of using the Galerkin-Spline procedure as opposed to the more conventional central difference method has been to yield a finite difference stencil of similar basic structure but differing coefficients. The central difference approach would yield (4-10) and (4-11) with the coefficients  $(1 \pm ia_1)$  being changed to  $(\pm ia_1)$  and  $(4 \pm 2ia_1)$  being changed to  $(6 \pm 2ia_1)$ . The use of the Galerkin-Spline is reportedly<sup>9</sup> more accurate.

Equations (4-10) and (4-11) are of tri-diagonal form and are solved by the recursive relations obtained by an adaptation of the Gauss elimination method. The complete set of equations for both the x and y directions are:

x Direction

$$A = C = 1 - ia_1 \quad (4-14)$$

$$B_j = 4 + 2ia_1, \quad j = 2, 3, \dots, J-1 \quad (4-15)$$

$$B_1 = B_J = 2 + 3(1 - 0.5X_M^{-2})/X_m h \quad (4-16)$$

$$+ a_1(1 \mp 0.5X_M h + 0.25h(1 - 0.5X_M^{-2})X_M^{-1})i,$$

$$G_j = (1 + ia_1)(D_{j-1,k}^n + D_{j+1,k}^n) + (4 - 2ia_1)D_{j,k}^n, \quad (4-17)$$

$$E_1 = -C/B_1, \quad (4-18)$$

$$F_1 = G_1/B_1, \quad (4-19)$$

$$E_j = -C(A E_{j-1} + B_j)^{-1}, \quad j = 2, 3, \dots, J \quad (4-20)$$

$$F_j = (G_j - A F_{j-1})(A E_{j-1} + B_j)^{-1}, \quad j = 2, 3, \dots, J \quad (4-21)$$

$$U_{J+1,k}^{n+\frac{1}{2}} = 0, \quad (4-22)$$

$$D_{j,k}^{n+\frac{1}{2}} = E_j D_{j+1,k}^{n+\frac{1}{2}} + F_j, \quad j = J, J-1, \dots, 1. \quad (4-23)$$

The sequence of relations, Equations (4-14) to (4-23), when performed for  $k = 1, 2, \dots, K$ , comprises the first half of the fractional step method. It should be noted that all quantities are complex and that complex arithmetic is implied throughout.

y Direction

The algorithm for the y direction is similar to that for the x direction with changes arising due to the assumed line of symmetry.

$$A = C = 1 - ia_1, \quad (4-24)$$

$$B_k = 4 + 2ia_1, \quad k = 1, 2, \dots, K-1 \quad (4-25)$$

$$B_K = B_J \quad \text{Eq. (4-16)} \quad (4-26)$$

$$G_k = (1 + ia_1)(D_{j,k-1}^{n+\frac{1}{2}} + D_{j,k+1}^{n+\frac{1}{2}}) + (4 - 2ia_1)D_{j,k}^{n+\frac{1}{2}}, \quad (4-27)$$

$$E_1 = -2C/B_1, \quad (4-28)$$

$$F_1 = G_1/B_1, \quad (4-29)$$

$$E_k = -C(A E_{k-1} + B_k)^{-1}, \quad k = 2, 3, \dots, K \quad (4-30)$$

$$F_k = (G_k - A F_{k-1})(A E_{k-1} + B_k)^{-1}, \quad k = 2, 3, \dots, K \quad (4-31)$$

$$D_{j,K+1}^{n+1} = 0, \quad (4-32)$$

$$D_{j,k}^{n+1} = E_k D_{j,k+1}^{n+1} + F_k, \quad k = K, K-1, \dots, 1. \quad (4-33)$$

Upon completion of this second half of the alternating direction method, the array  $D_{jk}^n$  has been replaced with  $D_{jK}^{n+1}$ . When combined with the phase initialization, Section VI, this operation advances the solution one step. A FORTRAN IV subroutine for this algorithm is listed in Appendix B.

## V. FAST FOURIER TRANSFORM METHOD

Fast Fourier Transform algorithms have been employed for solving boundary value problems by a number of investigators.<sup>25-27</sup> These efforts involved the use of the FFT to reduce the dimensionality of certain difference equations, the resulting numerical methods requiring a mixed procedure entailing aspects of the more traditional implicit difference schemes as in Section IV. An FFT algorithm for solving the atmospheric propagation problem for collimated beams was proposed by Wallace,<sup>19</sup> and led to the effort being reported here and in the MICOM report<sup>22</sup> previously mentioned. An FFT algorithm for propagation within a laser cavity is described by Canavan and Phelps.<sup>20,21</sup> The authors report on one method applicable to collimated beams which utilize the Helmholtz equation as a point of departure. A second technique is reported which is applicable for diverging beams and which makes use of the paraxial approximation. This latter form contains a singularity at  $z=0$  and does not seem to be generally applicable. The algorithm proposed by Wallace<sup>19</sup> is designed for the solution of the paraxial equation for collimated beams and is based on a forward difference approximation in the Z direction. This algorithm would march one step of the solution to Equation (2-16) by the three-stage operation

$$\bar{U}(p,q,Z) = \text{FFT}[U(x,Y,Z)e^{i\beta\mu\Delta Z}], \quad (5-1)$$

$$\bar{U}(p,q,Z + \Delta Z) = \bar{U}(p,q,Z)[1 + i\Delta Z(p^2 + q^2)/2]^{-1}, \quad (5-2)$$

$$U(x,Y,Z + \Delta Z) = \text{FFT}_I[\bar{U}(p,q,Z + \Delta Z)], \quad (5-3)$$

where the symbolism FFT and  $\text{FFT}_I$  indicate operation on a two-dimensional array of complex data by the forward and inverse FFT algorithm. This algorithm, while being competitive with existing methods, suffers the disadvantage of requiring a Nyquist-type accuracy criterion. For example, when  $\mu=0$  (vacuum propagation), the exact FFT transform solution to (2-16) requires that in (5-2)  $\bar{U}$  be given by

$$\bar{U}(p,q,Z + \Delta Z) = \bar{U}(p,q,Z)e^{-i\Delta Z(p^2 + q^2)/2}. \quad (5-4)$$

Since this solution is cyclic, the Nyquist criterion indicates that a minimum of six samples per cycle is needed to integrate a harmonic of a particular frequency. When Equation (5-2) is used, the Nyquist criterion, when applied to the highest frequency ( $\pi/\Delta x = \pi/\Delta y$ ), leads to

$$\Delta Z \leq 2\Delta x^2/3\pi. \quad (5-5)$$

For the IGS method Herrmann and Bradley suggest the forward marching be governed by the step-size criterion,  $\Delta Z = \Delta x^2$ , which is approximately one sample per cycle for the Nyquist frequency. As they show, however, this criterion does lead to sizable but tolerable phase errors at the high frequencies. Hence, in (5-5) and (5-2) one could similarly sacrifice the accuracy of the high-frequency components by relaxing (5-5). From this the conclusion can be drawn that the algorithm given by (5-1) to (5-3) requires a step-size criterion that is similar to the IGS method but differs by a factor near unity to be determined by numerical experiment. The two algorithms thus differ in their cost according to their relative cost in marching the solution one step forward, other factors being assumed equal. As will be detailed in a later section, the single-step IGS algorithm is about 15 percent faster than the FFT as executed on BRL's BRLESC II computer. In contrast, it will be shown by example that the FFT algorithm is more accurate for a specified grid size than is the IGS method.

By analogy with the algorithm to be described in a later section, the above algorithm can be made more attractive by replacing (5-2) with (5-4). This can be justified by virtue of the approximation

$$e^{-i\Delta Z(p^2 + q^2)/2} \approx [1 + i\Delta Z(p^2 + q^2)/2]^{-1} \quad (5-6)$$



or by assuming constancy of  $\mu$  within a step  $\Delta z$ . By this artifice the Nyquist requirement is eliminated; however, the algorithm can be shown to propagate the non-linear effect to an accuracy that is first-order accurate in  $\Delta z$ .

In order to obtain a more accurate algorithm, to eliminate the need for the Nyquist criterion, and, more importantly, to handle focused as well as collimated beams, we derive an FFT algorithm utilizing the sequence of transformations in Section III.

The FFT algorithm is also designed to advance the solution to Equation (3-9) in stages from plane  $z_n$  to  $z_{n+1}$ , each stage preceded by a phase initialization. For reasons peculiar to FFT computer subroutines we do not use the line of symmetry but work on the rectangle

$$\begin{aligned} -X_M \leq x \leq X_M, \\ -Y_M \leq y \leq Y_M, \end{aligned} \quad (5-7)$$

with the grid points as defined by (4-2). On this region, at the arbitrary plane  $z$ , the complex wave function  $D$  is assumed to have a Fourier series approximation

$$D(x, y, z) = \sum_{j=1}^J \sum_{k=1}^K d_{jk}(x, y, z), \quad (5-8)$$

where

$$d_{jk}(x, y, z) = C_{jk}(z) \exp(ip_j x + iq_k y). \quad (5-9)$$

By assuming that each component of the series satisfies (3-9) in the interval  $(z_n, z_{n+1})$ , we guarantee that (5-8) also is a solution. Hence, the amplitude of each harmonic for advancing from  $z_n$  to  $z_{n+1}$  is given by

$$C_{jk}(z_{n+1}) = C_{jk}(z_n) \exp[-\frac{1}{2} i \Delta z (p_j^2 + q_k^2)], \quad (5-10)$$

where, because of the transformations leading to (3-9), we solve the one-step propagator "exactly." From the theory of finite Fourier series for discrete data it can be shown that

$$C_{jk}(z_n) = (JK)^{-1} \sum_{\ell=1}^J \sum_{m=1}^K D(x_\ell, y_m, z_n) \exp(-ip_\ell x_j - iq_m y_k), \quad (5-11)$$

where

$$p_\ell = \begin{cases} 2\pi(\ell - 1)/(J\Delta x), & \ell = 1, 2, \dots, J/2 \\ 2\pi(\ell - 1 - J)/(J\Delta x), & \ell = J/2 + 1, \dots, J \end{cases} \quad (5-12)$$

$$q_m = \begin{cases} 2\pi(m-1)/(K\Delta y), & m = 1, 2, \dots, K/2 \\ 2\pi(m-1-K)/(K\Delta y), & m = K/2+1, \dots, K. \end{cases} \quad (5-13)$$

The inverse finite Fourier transform at level (n+1) is given by

$$D(x, y, z_{n+1}) = \sum_{j=1}^J \sum_{k=1}^K C_{jk}(z_{n+1}) \exp(ip_j x + iq_k y). \quad (5-14)$$

The operations defined by the sums in (5-11) and (5-14) can be related to the operations performed by the so-called Fast Fourier Transforms. See Appendix A. In (5-11) and (5-14) we have adopted a convention which "folds" the negative frequencies to the second half of the series. This form is compatible with the convention used in most computer subroutines. See, for example, Brenner.<sup>28</sup>

## VI. PHASE INITIALIZATION

The employment of the phase transformation (3-6), (3-7) is equivalent to propagating one  $z$  increment holding the phase distribution fixed at what is anticipated will be the distribution at the middle of the step. This "anticipation" is implemented by assuming that the function  $g$  can be separated into similarity type products of functions depending on  $z$  and on  $x, y$ . In this manner the  $z$  dependence can be accounted for by quadrature, and within the half step the  $x, y$  dependence is assumed to be similar to the behavior at the beginning of the step. Once the step has been taken, by application of the basic algorithm, the phase of the wave function is now "off" by one-half step. The phase is updated by again assuming separability of  $g$  and similarity, this time, however, using the  $x, y$  dependence of  $g$  calculated at the end of the step. This phase updating can be combined with the phase initialization for the next half step and done in one operation. If the scaling parameter  $a$  is completely arbitrary--that is, its slope is discontinuous at each step--then an additional phase increment must be included. These operations are defined in the equations that follow. We let

$$\Gamma(x, y, z) = \int_{z_{n+1/2}}^z [f_1(Z)\bar{u}(x, y, z) + f_2(Z)(x^2 + y^2)] dz, \quad (6-1)$$

where

$$f_1(Z) = 2\alpha\beta\gamma a [Z(z)] e^{-\alpha Z} [1 + \omega Z(z)]^{-1}, \quad (6-2)$$

$$f_2(Z) = -\beta^2 a^3 \partial^2 a / \partial Z^2, \quad (6-3)$$

and

$$\bar{u}(x, y, z) = - \int_{-\infty}^x |D(x, y, z)|^2 dx. \quad (6-4)$$

The phase updating is accomplished by multiplying the "old" wave function by a complex phase increment and storing the "new" wave function over the old; that is

$$D_{\text{new}}(x, y, z_n) = D_{\text{old}}(x, y, z_n) e^{-i\Delta\phi}, \quad (6-5)$$

where

$$\Delta\phi = \frac{1}{2} \bar{\mu}(x, y, z_n) (E_n + F_n) \quad (6-6)$$

$$+ \frac{1}{2} (x^2 + y^2) (G_n + H_n + I_n + J_n),$$

$$E_n = - \int_{z_n - \frac{1}{2}\Delta z_{n-1}}^{z_n} f_1(Z) dz, \quad (6-7)$$

$$F_n = \int_{z_n + \frac{1}{2}\Delta z_n}^{z_n} f_1(Z) dz, \quad (6-8)$$

$$G_n = - \int_{z_n - \frac{1}{2}\Delta z_{n-1}}^{z_n} f_2(Z) dz, \quad (6-9)$$

$$H_n = \int_{z_n + \frac{1}{2}\Delta z_n}^{z_n} f_2(Z) dz, \quad (6-10)$$

$$I_n = - \left. \beta a(Z_n) \partial a / \partial Z \right|_{Z=Z_n^-}, \quad (6-11)$$

$$J_n = \left. \beta a(Z_n) \partial a / \partial Z \right|_{Z=Z_n^+}. \quad (6-12)$$

In the computer code the four integrals (6-7) to (6-10) are done by trapezoidal quadrature. When the scaling length  $a$  has a continuous slope in going from step to step, the sum  $(I_n + J_n)$  vanishes.

## VII. CHOICE OF SCALING LENGTH FOR ADAPTIVE COORDINATES

The scale length  $a(Z)$  used in defining the adaptive coordinates is present in the phase transformation (3-2). The initial wave function after transformation is given by

$$B(x, y, 0) = a f(ax, ay) e^{i(\phi + \phi_1)} \quad (7-1)$$

where

$$\phi_1(x, y, 0) = -\frac{1}{2} (x^2 + y^2) (\beta \partial a / \partial Z |_{Z=0} + \beta_1). \quad (7-2)$$

Unless  $a(Z)$  is properly chosen,  $\phi_1$  can become quite large away from the center of the beam, leading to rapid oscillations in the initial data. Such oscillations, to be sampled adequately, would require too fine a mesh size for practical computation. The manner in which this difficulty is avoided is described below for focused beams and collimated beams.

### Focused Beams

For focused beams  $\beta_1 = \beta$  in Equation (7-2). Hence, if  $\partial a / \partial Z = -1$  at  $Z = 0$ ,  $\phi_1$  will be identically 0 as desired. The choice of

$$a(Z) = [1 - Z]^2 + (Z/\beta)^2 \quad (7-3)$$

by Herrmann and Bradley<sup>9</sup> and by Ulrich<sup>13</sup> has this advantage but suffers the disadvantage of focusing as does a beam in vacuum, thus not allowing enough grid space for severely bloomed beams. The choice of

$$a = 1 - (1 - N/\beta)Z \quad (7-4)$$

is similar to Aitken et al. and has the advantage of being  $N$  times diffraction limited at the focus. Here  $N$  can be chosen arbitrarily, depending on the expected severity of thermal blooming. This choice has the disadvantage that  $\phi_1$  does not vanish completely; that is

$$\phi_1(x,y) = N(x^2 + y^2)/2. \quad (7-5)$$

Hence, if the  $N$  required to contain the bloomed beam is too large, this formulation may lead to a poor numerical solution. This is apparent in Problems 1 and 2 for an  $N$  of 5. The above two candidates assume that one formula governs the  $z$  variation of  $a$  from aperture to focus. This requires that  $z_0$  in Equation (3-3) be zero. A generalization of this choice is to advance to the focus in a manner where  $a(z)$  is piecewise linear. In this way,  $a$  can have an initial slope of  $-1$ , thus nulling  $\phi_1$ , and can be gradually varied at each step so as to have the proper scaling according to the demands of the blooming. Here we have

$$a(Z) = a_n + b_n(Z - Z_n), \quad Z_n \leq Z \leq Z_{n+1}, \quad (7-6)$$

and

$$z = \beta^{-1} \int_{Z_n}^Z [a_n + b_n(Z - Z_n)]^{-2} dZ$$

$$= \begin{cases} (\beta b_n)^{-1} [a_n^{-1} - \{a_n + b_n(Z - Z_n)\}^{-1}], & b_n \neq 0 \\ (\beta a_n^2)^{-1} (Z - Z_n), & b_n = 0. \end{cases} \quad (7-7)$$

An additional attractive candidate for  $a$  is

$$a = 1 - Z + NZ^2/\beta. \quad (7-8)$$

It has the desired properties of -1 initial slope and arbitrary size at the focus. Its major disadvantage is that it does not permit the integral in (23) to be done in simple closed form.

The choice

$$a = [(1 - Z)^2 + (NZ/\beta)^2]^{1/2} \quad (7-9)$$

has all the requisite characteristics. This form is seen to be similar to the Z-dependent beam waist for a focused Gaussian beam with the scale gradually evolving to N times larger than that expected in vacuum. While this form seems to be an obvious generalization of the previously used<sup>9</sup> (7-3), the freedom to use the generalization is not readily apparent until one proceeds to perform the sequence of transformations as done in Sections III and VII. For a in (7-9), Equation (3-3) relating z and Z becomes

$$z = N^{-1} \tan^{-1} [NZ/\beta(1 - Z)], \quad (7-10)$$

and

$$Z = \beta \tan z / (N + \beta \tan z). \quad (7-11)$$

The two equations (7-10) and (7-11) thus permit the integration or marching to proceed in z space while simultaneously computing such quantities as  $f_1(Z)$  and  $f_2(Z)$  which are more conveniently expressed in Z.

It should be noted that there are "tradeoffs" among these various choices. For example, when  $a(Z)$  is piecewise linear, its second derivative vanishes, eliminating one term in the phase function  $g(z)$ , but introduces an additional term because of the discontinuity. In Equation (7-9) the second derivative of a, as required in (3-5), takes the form

$$\partial^2 a / \partial z^2 = (N^2/\beta^2)/a^3. \quad (7-12)$$

#### Choice of $\Delta z$

Marching or integrating forward in steps of fixed  $\Delta z$  is good strategy since, through the transformations, the effect is to use more z planes in the region where the beam is tightly focused and fewer planes elsewhere. It can be shown that for  $a(Z)$  chosen by (7-4) the focus is reached when

$$z = 1/N. \quad (7-13)$$

Hence, if we elect to march to the focus in M equal steps,  $\Delta z$  is given by

$$\Delta z = 1/MN. \quad (7-14)$$

For  $a(Z)$  in (7-9) the focal z is equal to  $\pi/2N$  and

$$\Delta z = \pi/2MN. \quad (7-15)$$

In order to have a flexible code the author's codes have been designed to allow optionally for fixed  $\Delta z$  or fixed  $\Delta Z$  with provisions for a maximum  $\Delta Z$  when  $\Delta z$  is fixed.

### Collimated Beams

For collimated beams  $\beta_1$  in Equation (7-2) is zero. If the computations are done without an adaptive coordinate system,  $\partial a / \partial Z = 0$  and  $\phi_1$  is identically zero. If the blooming is severe enough to spread the beam beyond the original coordinate system, the linear form of  $a$ , Equation (7-4), is generally adequate. If the required  $N$  is not too large (2 or 3), then the oscillations can be adequately sampled. A seemingly better choice (though not tried) is

$$a(Z) = 1 + dZ^2. \quad (7-16)$$

The term  $\phi_1$  vanishes for this choice and

$$z = Z(2d^2 + 2dZ^2)^{-1/2} + (2d)^{-1/2} \tan^{-1}(z/d^{1/2}). \quad (7-17)$$

This form requires marching in steps of fixed  $Z$ , since inverting of (7-14) to reference  $z$  dependent quantities requires a numerical procedure. The parameter  $d$  is free to be chosen according to the thermal blooming that is expected.

## VIII. A COMPARISON OF THE ACCURACY AND EFFICIENCY OF THE TWO METHODS

The two algorithms were compared employing two different methods for choosing the adaptive coordinates and utilizing different step size  $\Delta z$ . Two sample problems were done, one with a "small" Fresnel number of 2.96 and the second with a "moderate" Fresnel number of 9.3. Both cases experience severe thermal blooming and tax the state of the art for such computations.

### Problem 1

The first problem is the so-called NRL sample problem. We assume an ideal Gaussian beam focused at a range of 2 km. The parameters are given by

$$f(\xi, \eta) = \exp\left[-\frac{1}{2} (\xi^2 + \eta^2)/r^2\right]$$

$$\alpha_1 = 0.064/\text{m}$$

$$P/V = 44.843 \text{ kw-sec/m}$$

$$r = 10 \text{ cm}$$

$$R = 2 \text{ km}$$

$$\Omega = 0.0/\text{sec}$$

$$\lambda = 10.6 \times 10^{-6} \text{ m}$$

$$\phi = .0$$

The parameters associated with the computations are as follows. For both methods the extent of the grid at the exit plane was  $\pm 4$  beam radii with symmetry utilized for the IGS method. An  $N$  of 5 was used for the coordinate system. For the IGS method the number of grid points was  $65 \times 33$  and  $64 \times 64$  for FFT. The actual size of the individual cells was essentially identical but twice as many cells were used for the FFT because of the requirements of the subroutine. With this gridding, one step of IGS was about 15 percent faster than one step of FFT. By implication, in problems not permitting the symmetry the FFT would be over 1.5 times faster than the IGS. Alternatively, special modification of the FFT subroutines would gain the same factor.

For this problem the number of  $z$  steps to the focus was varied to see if either method permitted more rapid advance. In Figures 1 through 4 the notations I and II are used to denote the strategy for choosing the adaptive coordinate system, the notation implying

I,  $a(z)$  determined by Equation (7-4),

II,  $a(z)$  determined by Equation (7-9).

For this problem we have compared only the peak intensity at the various ranges. The solid line in Figures 1-4 is the result obtained by Hogge<sup>5</sup> for the identical problem using an explicit difference scheme with a grid of  $121 \times 121$  in  $x, y$  and 247  $z$  planes. In order to compare with Hogge's result, we have multiplied the intensity by  $e^{\alpha z}$  to conform with his convention (private communication).

In Figures 1 and 2, the IGS method is seen to agree closely with Hogge for 10  $z$  steps, but for 5  $z$  steps and  $a(z)$  chosen by I the IGS method is off considerably. For the FFT method, Figures 3 and 4, the results again agree very well; but, most importantly, the solution shows almost no sensitivity to relaxing  $\Delta z$  to 5 steps when choosing  $a(z)$  by either I or II. No attempt was made to solve this problem with either method for less than 5 steps. Neglecting the solutions using I, the results for this problem are inconclusive. However, we note that we neglected the usual step-size criterion in the IGS method. We would therefore conclude that for this problem the two methods are comparable only if we know *a priori* that the step-size criterion can be ignored. In Problem 2 we will show that it cannot in general be ignored for IGS but can be for the FFT.

#### Problem 2

The second problem has more severe thermal blooming than Problem 1. Again we consider an ideal Gaussian beam focused at 2 km. The parameters for this problem are

$$\alpha_1 = 0.224/\text{m}$$

$$P/V = 50 \text{ kw-sec/m}$$

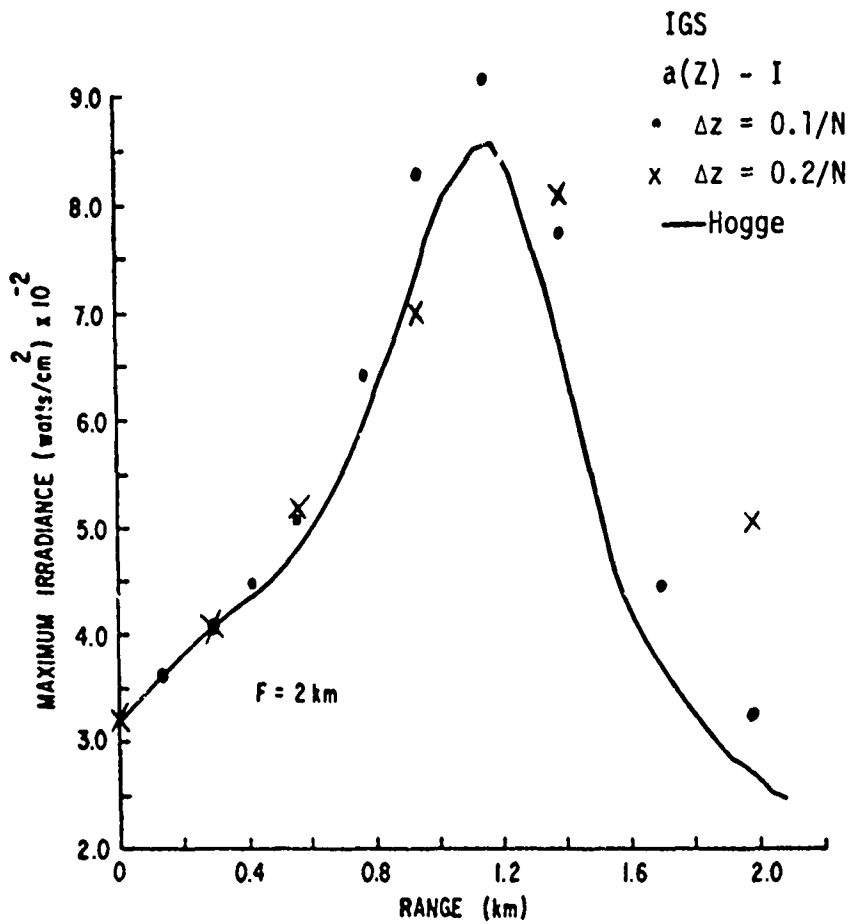


Figure 1. Problem 1 - Effect of Changing  $\Delta z$  for IGS Method



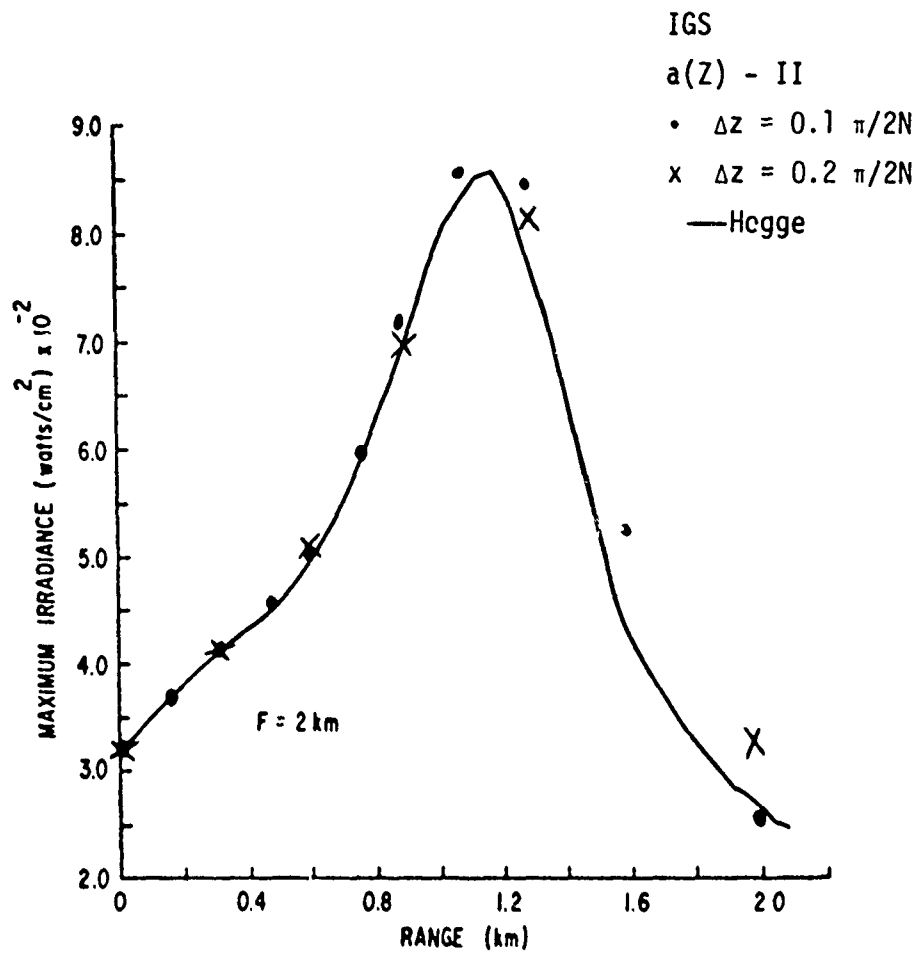


Figure 2. Problem 1 - Effect of Changing  $\Delta z$  for IGS Method

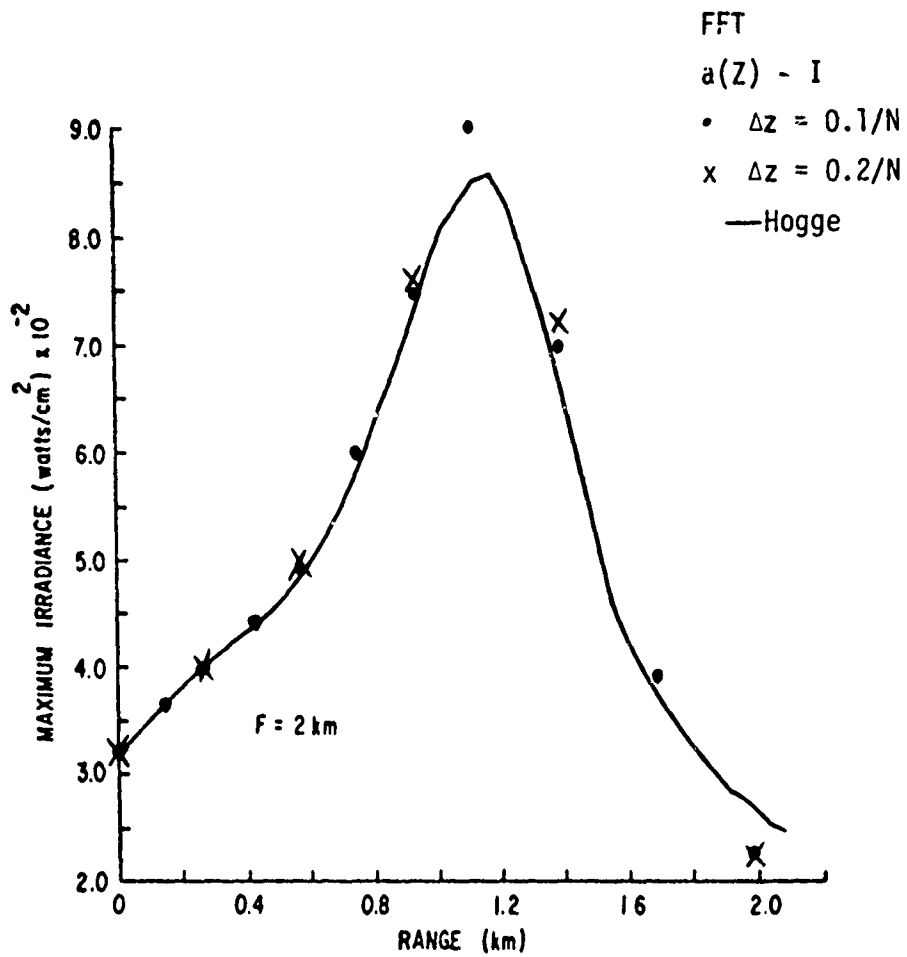


Figure 3. Problem 1 - Effect of Changing  $\Delta z$  for FFT Method

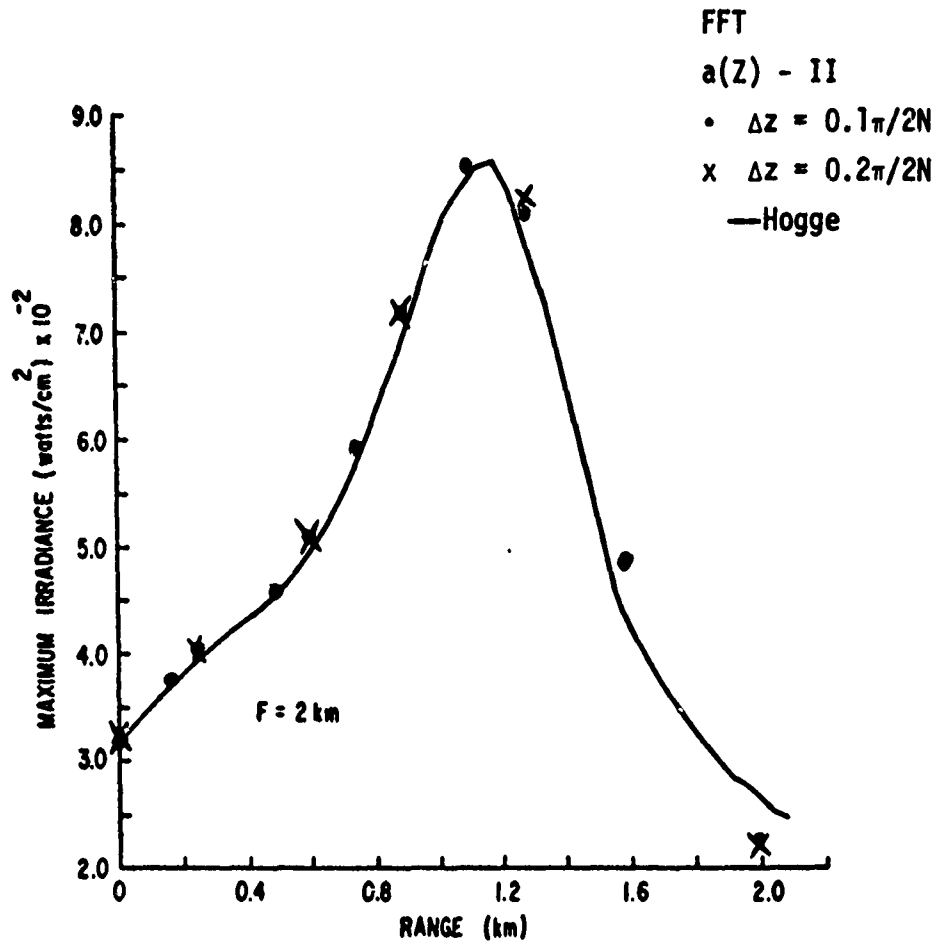


Figure 4. Problem 1 - Effect of Changing  $\Delta z$  for FFT Method

$$\begin{aligned}
r &= 25/\sqrt{2} \text{ cm} \\
R &= 2 \text{ km} \\
\Omega &= 0.0/\text{sec} \\
\lambda &= 10.6 \times 10^{-6} \text{ m} \\
N &= 5
\end{aligned}$$

The problem was solved utilizing both methods, two strategies for the adaptive grid, and various choices of  $\Delta z$ . The summary of the focal plane data and the key parameters used for each of the nine cases are listed in Table I. Figure 5 denotes the iso-irradiance contours at the aperture plane for each of the nine cases. The focal plane iso-irradiance contours obtained by using a subroutine developed by Hartwig<sup>29</sup> are contained in Figures 6-14. In these figures the point of peak intensity is denoted with an x, and the ratio of focal plane to aperture plane peak intensity is denoted as MAX FLUX. The intensity for each contour line is in decreasing increments of 0.1 times the peak intensity as one moves away from the x. The dashed circle is the  $e^{-1}$  contour for vacuum propagation and for no thermal blooming encompasses the first six contours. In the focal plane the extent of the computing grid is the original factor of 4 beam radii (4 times the small circle) times the factor of  $N=5$  to allow for blooming. The magnitude of the focal plane blooming is evident by comparing the area of the inner six contours with the small dashed circle in Figures 6-14.

Since the problem has no independent solution by which we can gauge the accuracy of the numerical solution, we have taken the usual approach of trying to find a region in mesh spacing where the solution is not sensitive. From experience, accurate solutions can be delineated by examination of the degree of smoothness in the iso-irradiance contours. Employing these two factors, we have made the judgment that the cases denoted with the symbol ++ are acceptable and accurate. It should be noted that, since the peak intensity is a quantity determined at a discrete point, some discrepancy between methods is to be expected, depending on the coarseness of the grid.

For this problem it was found that a grid of  $65 \times 33$  was not sufficient to obtain an accurate solution by the IGS method, Figures 6 and 8. For a grid of  $101 \times 51$  with the IGS method and  $a(Z)$  chosen by II (Figure 9), the solution at the focal plane agreed with the FFT cases using a grid of  $64 \times 64$ . For the IGS method it was found that using the step-size criterion  $\Delta z = \Delta x^2$  yielded an accurate solution (Figure 9), but when this restriction was ignored and 10 z steps were used (Figure 11) an inaccurate solution resulted. For the FFT method no appreciable difference resulted between 10 z steps and 5 z steps, Figures 13 and 14. The contrasting behavior of the two methods when  $\Delta z$  is increased is attributed to the Nyquist-type accuracy criterion as discussed in Section V. Even though implicit schemes are generally considered to be unconditionally stable, because of the cyclic nature, the Nyquist

TABLE I

## SUMMARY OF KEY PARAMETERS FOR PROBLEM 2

Figure No.	Method	Choice of $a(z)$	No. of $x, y$ Grid Pts.	No. of $z$ Steps	Peak Intensity*	Deflection <sup>†</sup>	Computing Time Minutes	
							Graphics	No Graphics
6	IGS	I	65 x 33	13**	2.15	-0.74	2.67	1.80
7	IGS	I	101 x 51	32**	1.60	-1.41	10.66	8.57
8	IGS	II	65 x 33	21**	1.30	-1.57	3.61	2.74
9	IGS	II	101 x 51	50**	.77**	-1.49	15.44	13.35
10	IGS	II	65 x 33	10	1.88	-1.18	2.36	1.49
11	IGS	II	101 x 51	10	1.96	-1.12	4.89	2.80
12	FFT	I	64 x 64	10	.96**	-1.41	2.64	1.77
13	FFT	II	64 x 64	10	.84**	-1.43	2.65	1.77
14	FFT	II	64 x 64	5	.80**	-1.44	1.97	1.10

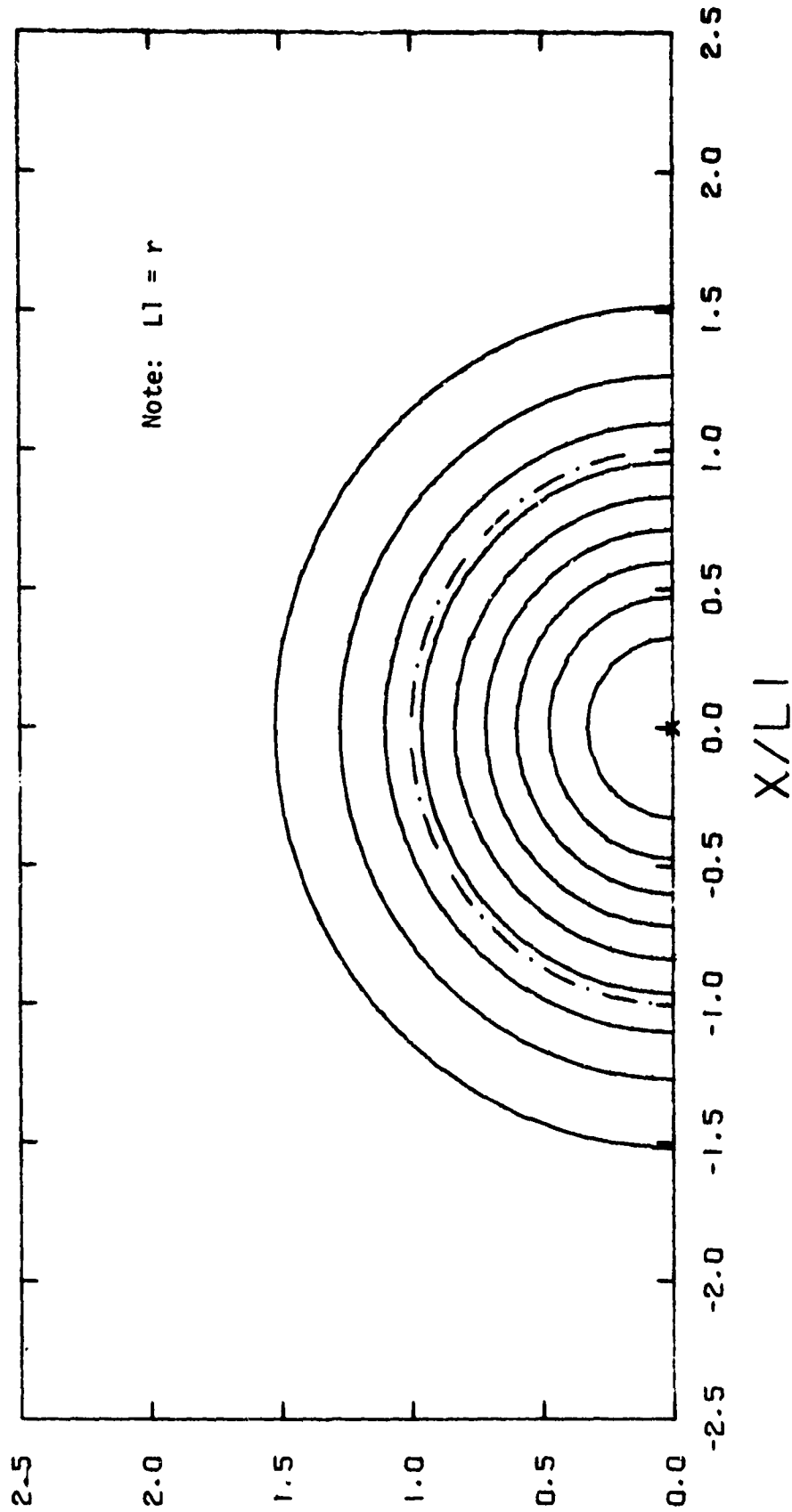
\* Denotes ratio of focal plane maximum intensity over aperture maximum.

† Denotes displacement of maximum intensity measured in units of  $r$ .

\*\* Denotes use of step-size criterion  $\Delta z = \Delta x^2$ .

\*\* Denotes acceptable solutions.

RUN NO. 721      ALPHA = 0.4480  
 Z/L2 = 0.00      BETA = 9.2618  
 MAX. FLUX = 1.00      GAMMA = 44.0375

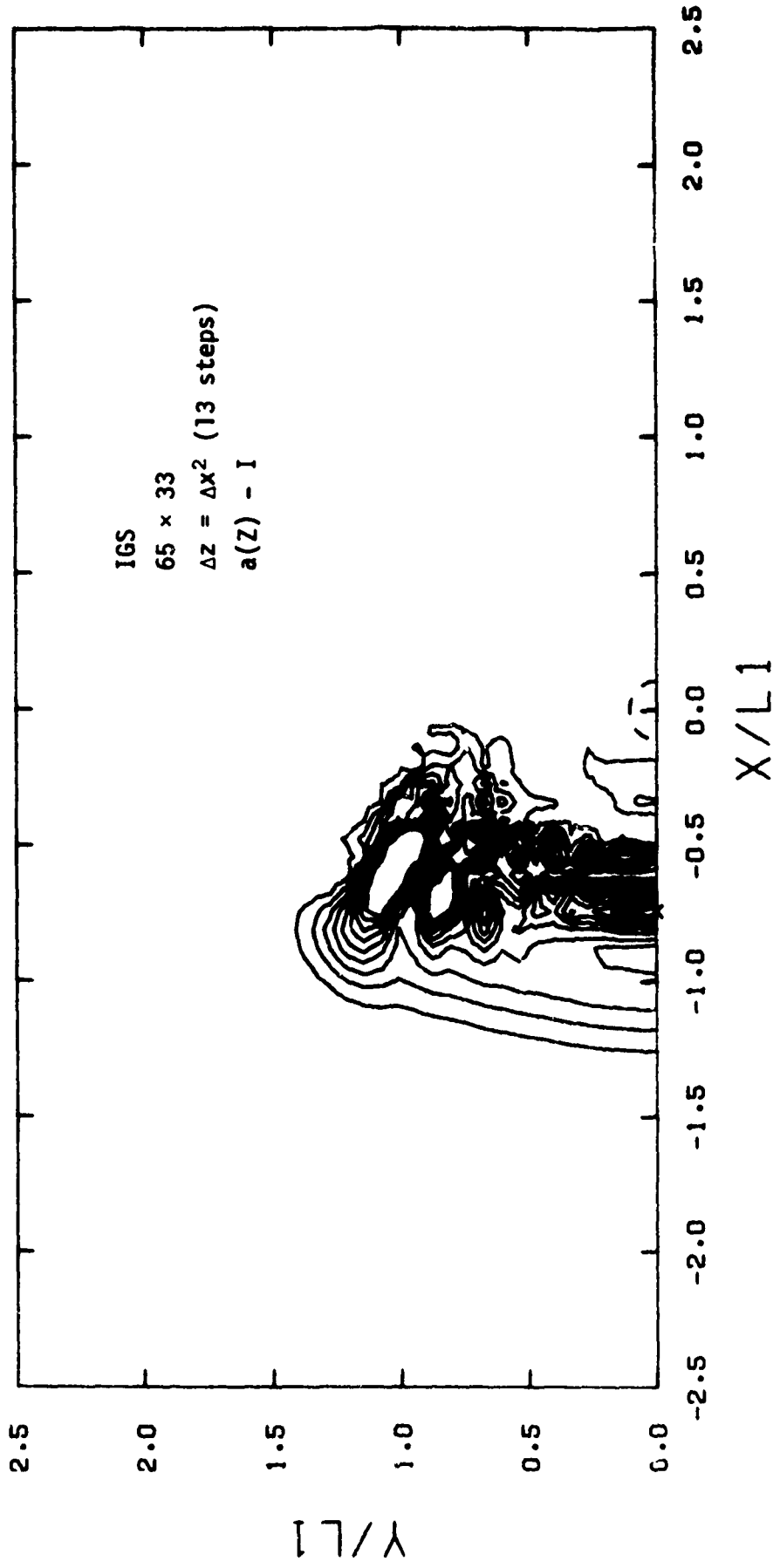


### ISO - IRRADIANCE CONTOURS

Figure 5. Aperture Plane Contours - Same for All Nine Cases

Y/L1

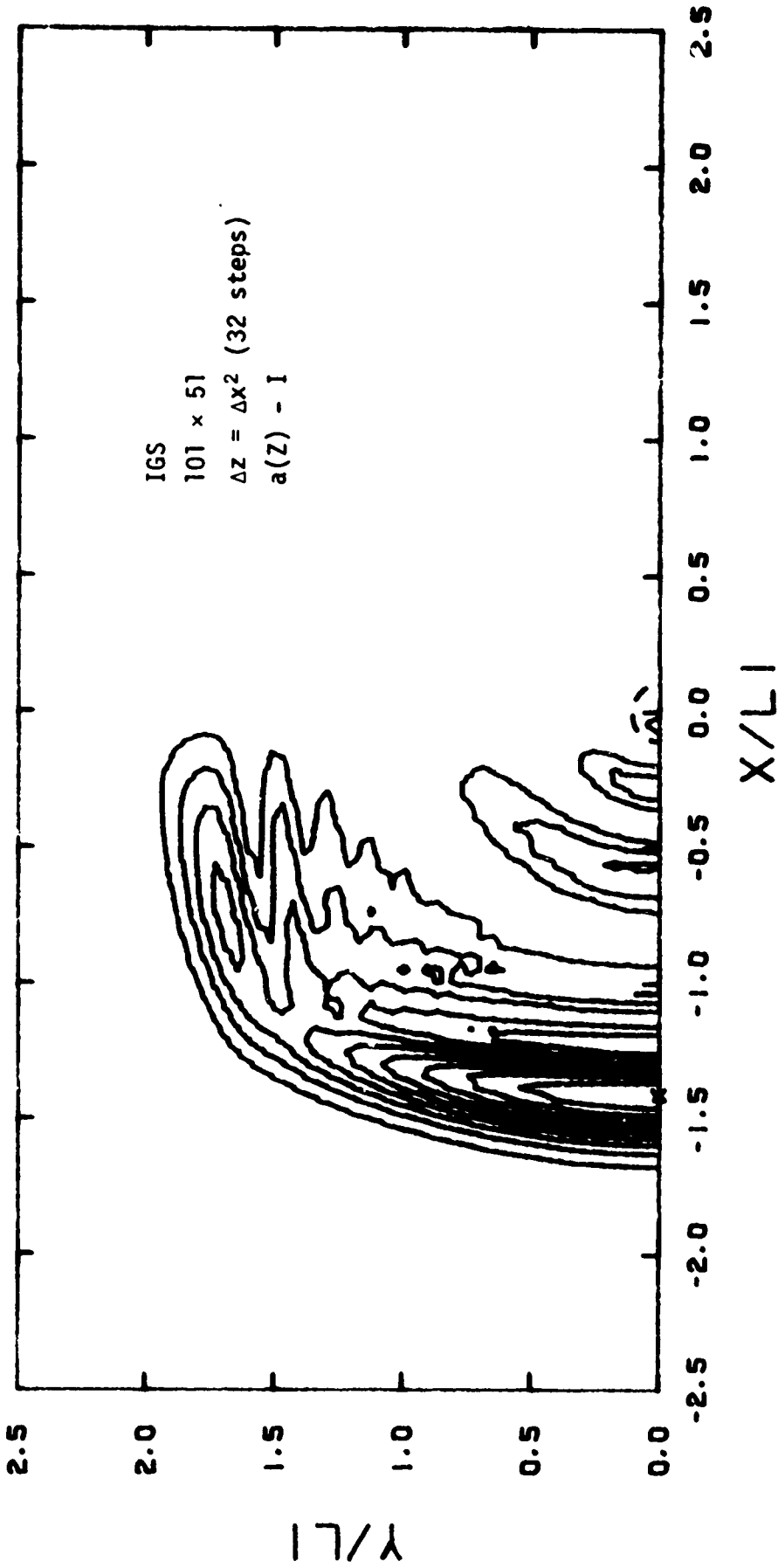
RUN NO. 718  
Z/L2 = 1.00  
MAX.FLUX= 2.15  
ALPHA = 0.4480  
BETA = 9.2618  
GAMMA = 44.0375



# ISO-IRRADIANCE CONTOURS

Figure 6. IGS Method - Grid Too Coarse - Phase Oscillations Not Removed

RUN NO. 718      ALPHA = 0.4480  
 Z/L2 = 1.00      BETA = 8.2616  
 MAX. FLUX = 1.60      GAMMA = 44.0375

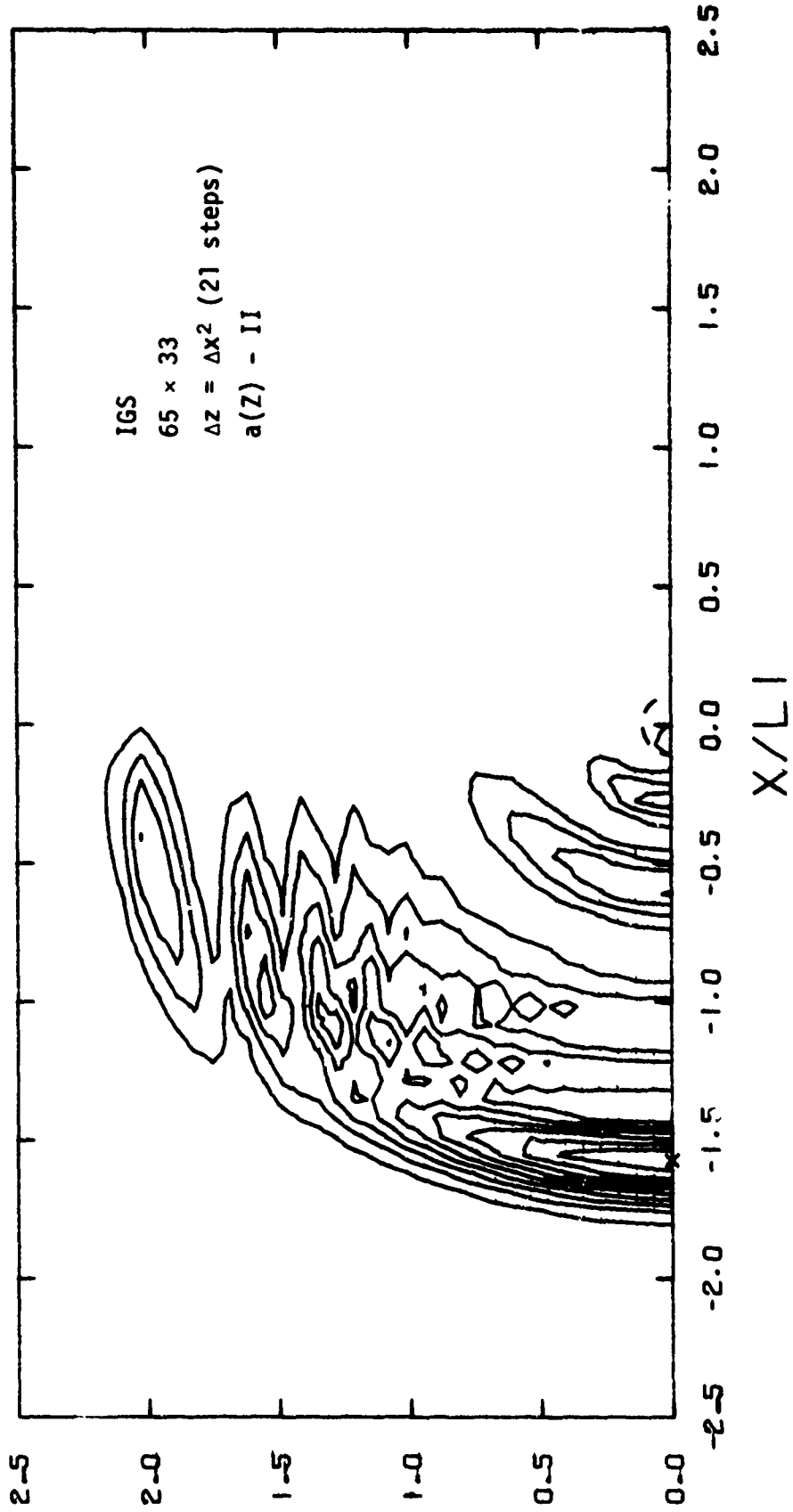


## ISO-IRRADIANCE CONTOURS

Figure 7. IGS Method - Phase Oscillations Not Removed



RUN NO. 720  
 Z/L2 = 1.00  
 MAX. FLUX = 1.30  
 ALPHA = 0.4480  
 BETA = 9.2618  
 GAMMA = 44.0375

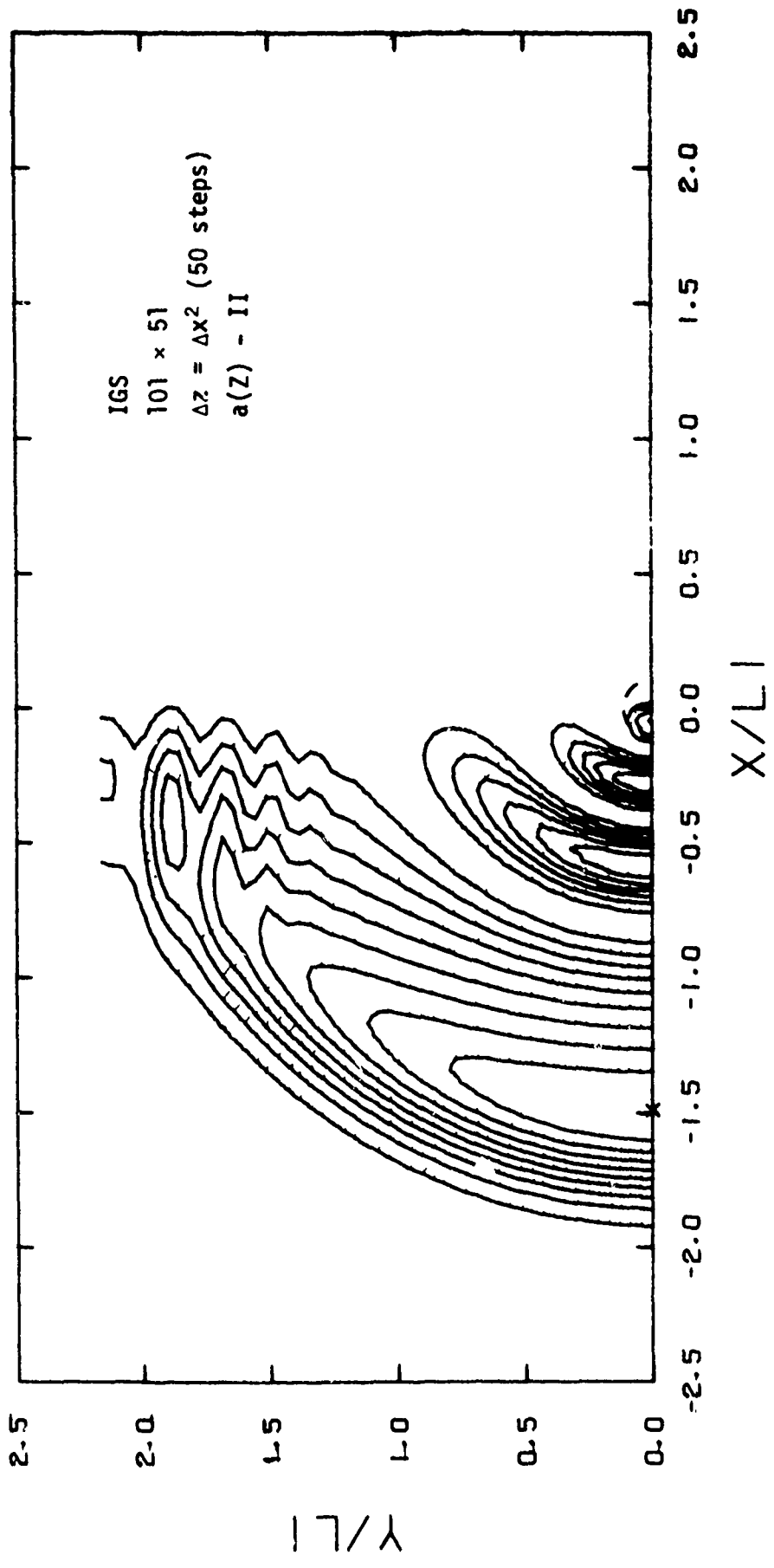


## ISO-IRRADIANCE CONTOURS

Figure 8. IGS Method - x,y Grid Too Coarse

Y/L1

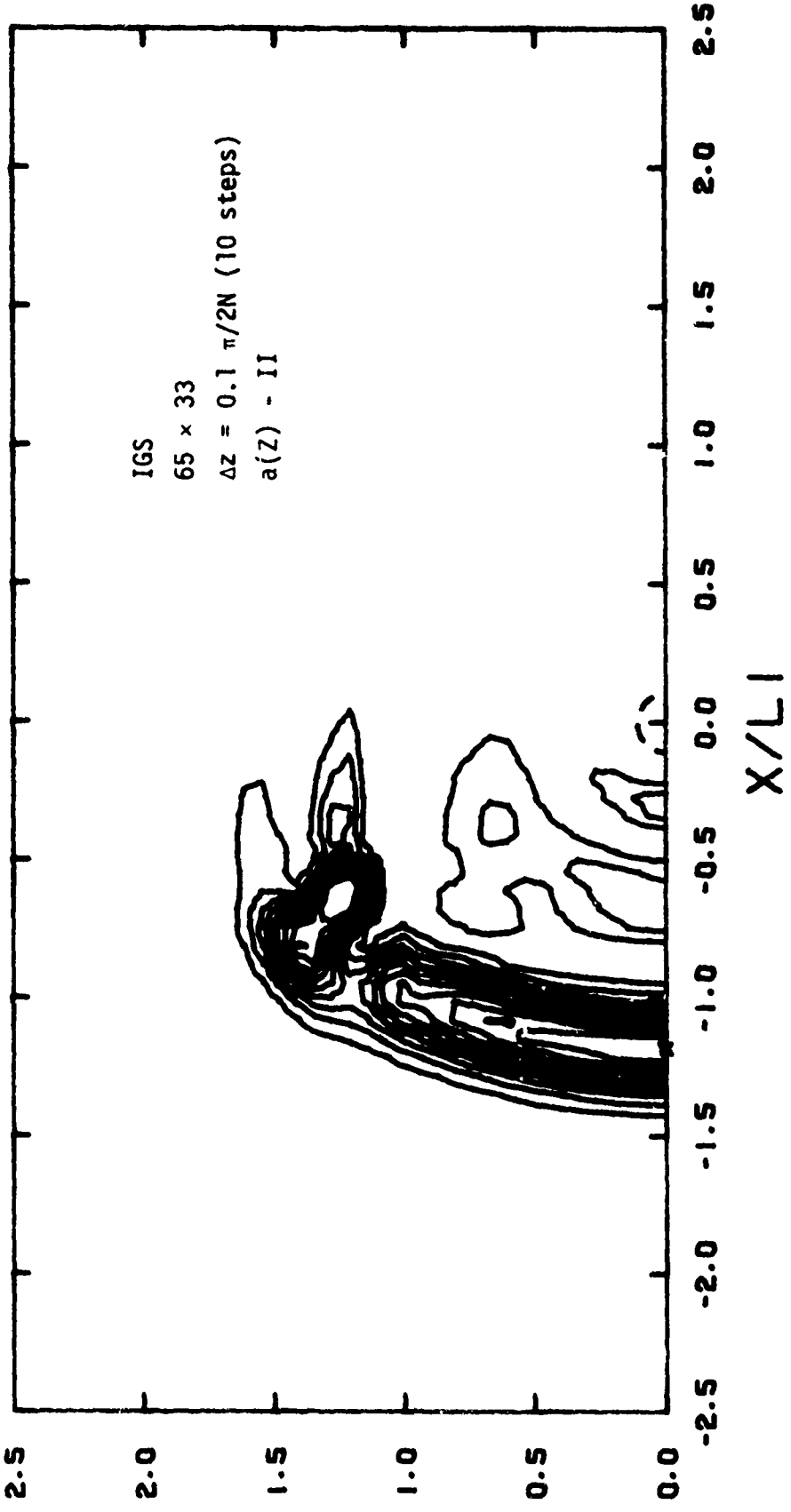
RUN NO. 721      ALPHA = 0.4480  
 Z/L2 = 1.00      BETA = 9.2618  
 MAX.FLUX = 0.77      GAMMA = 44.0375



## ISO-IRRADIANCE CONTOURS

Figure 9. IGS Method - Phase Oscillations Removed - Finer Gridding

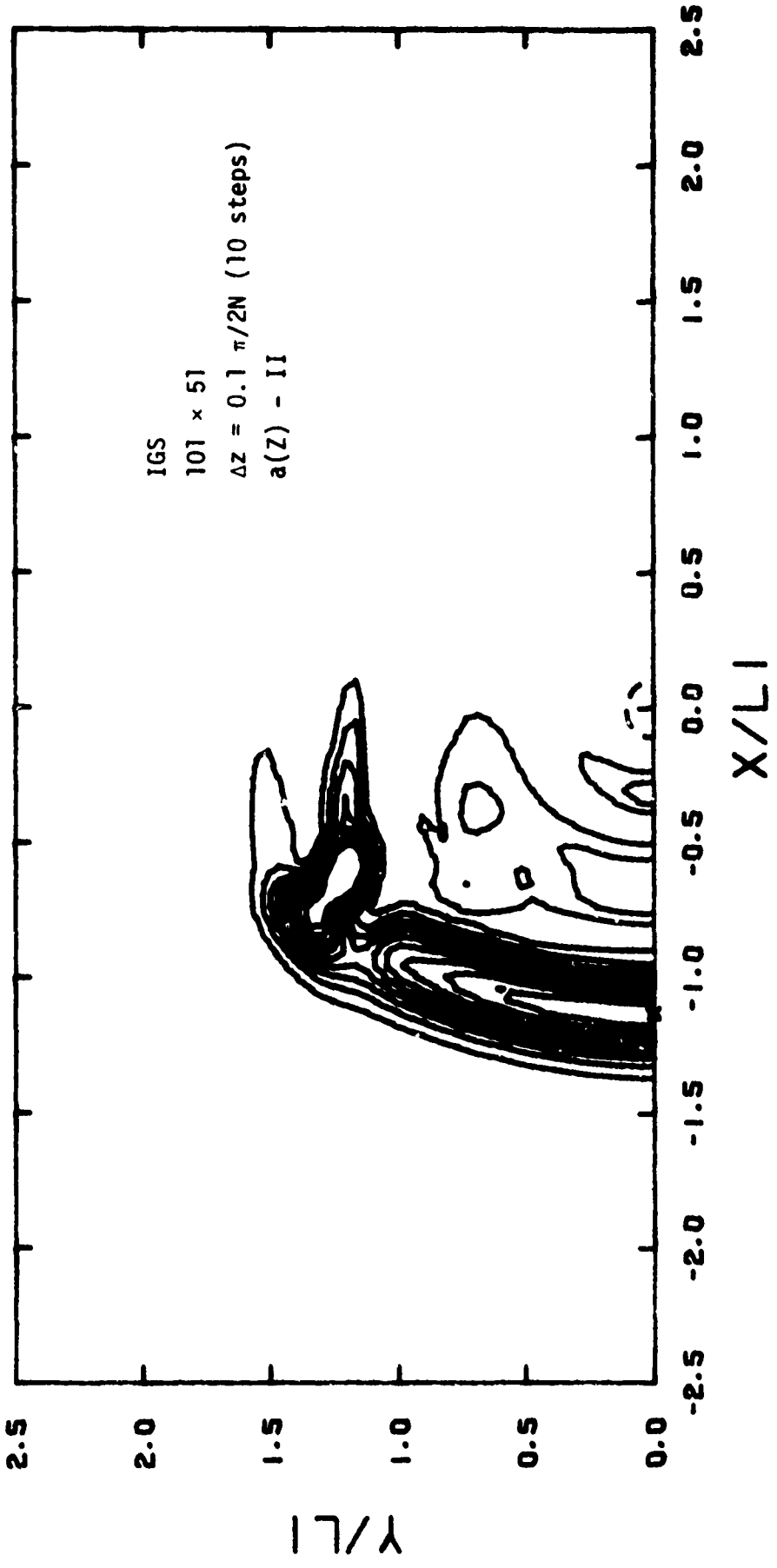
RUN NO. 724      ALPHA = 0.4460  
 Z/L2 = 1.00      BETA = 8.2616  
 MAX. FLUX = 1.68      GAMMA = 44.0375



## ISO-IRRADIANCE CONTOURS

Figure 10. IGS Method - Nyquist Criterion Ignored,  $\Delta z$  Too Large

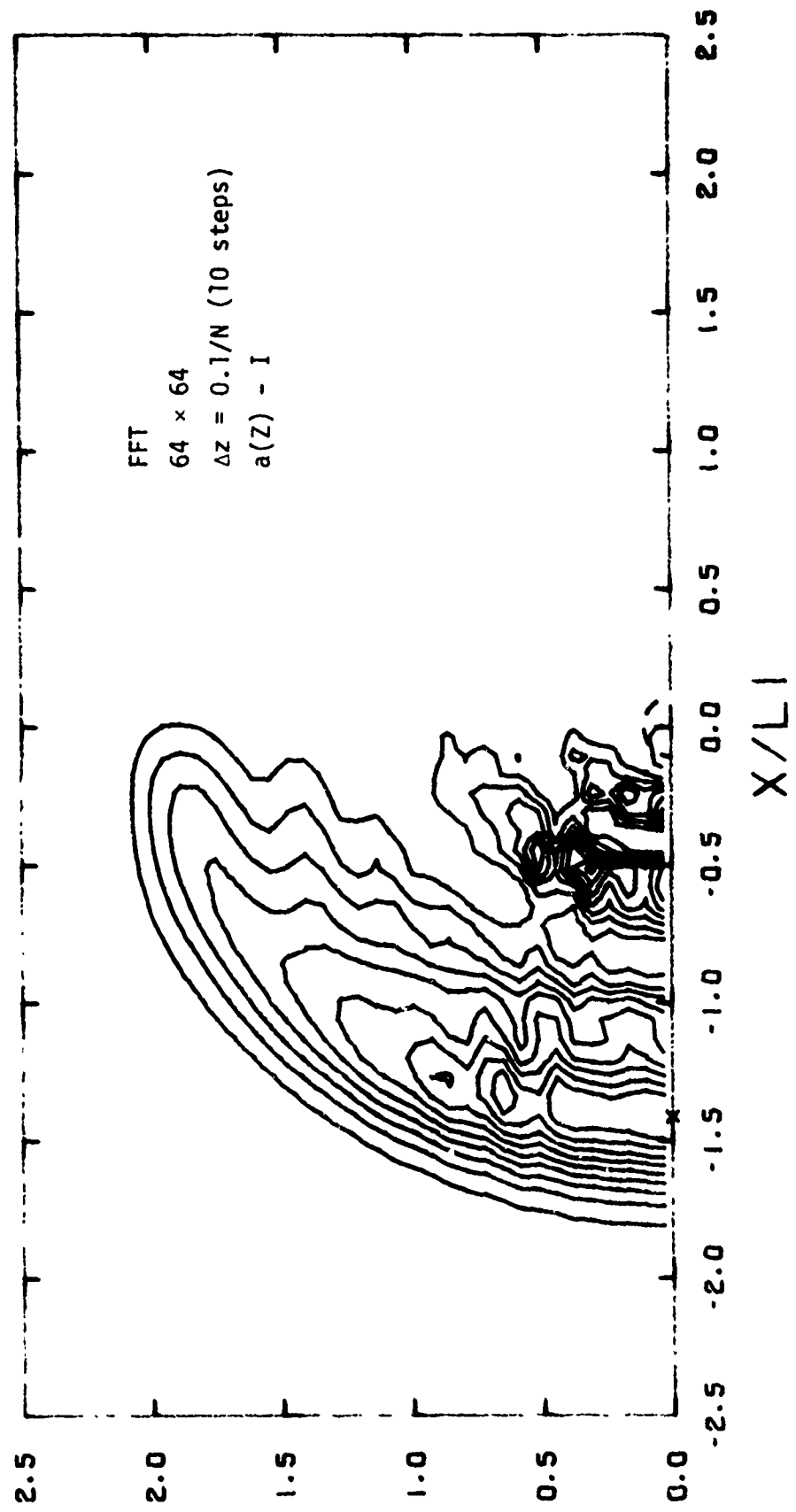
RUN NO. 725      ALPHA = 0.4460  
 Z/L2 = 1.00      BETA = 0.2616  
 MAX. FLUX = 1.96      GAMMA = 44.0375



## ISO-IRRADIANCE CONTOURS

Figure 11. IGS Method - Nyquist Criterion Ignored,  $\Delta z$  Too Large

RUN NO. 722      ALPHA • 0.4480  
 Z/L2 • 1.00      BETA • 9.2618  
 MAX.FLUX • 0.86      GAMMA • 44.0375

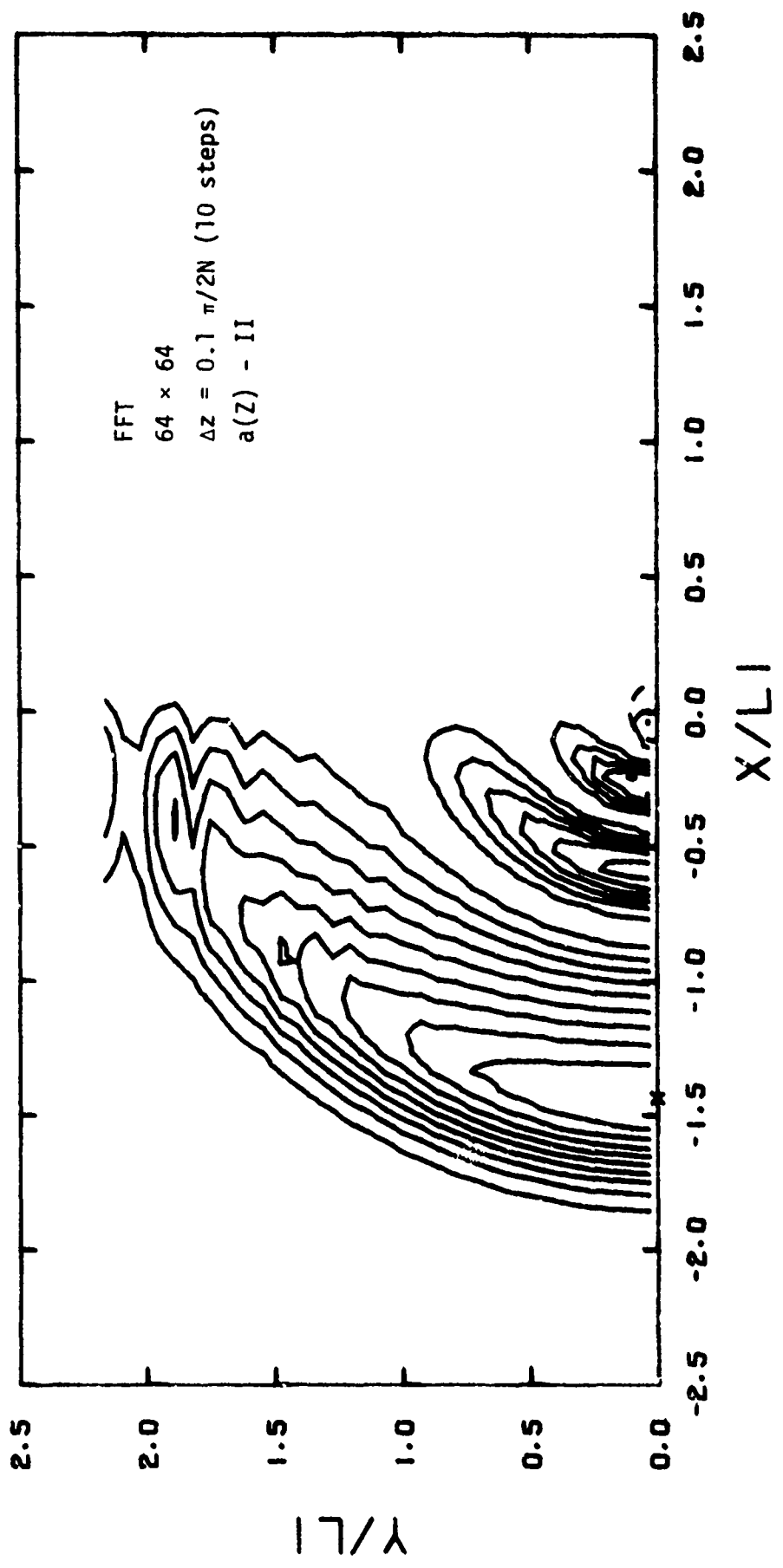


## ISO-IRRADIANCE CONTOURS

Figure 12. FFT Method - Phase Oscillations Not Removed

Y/L1

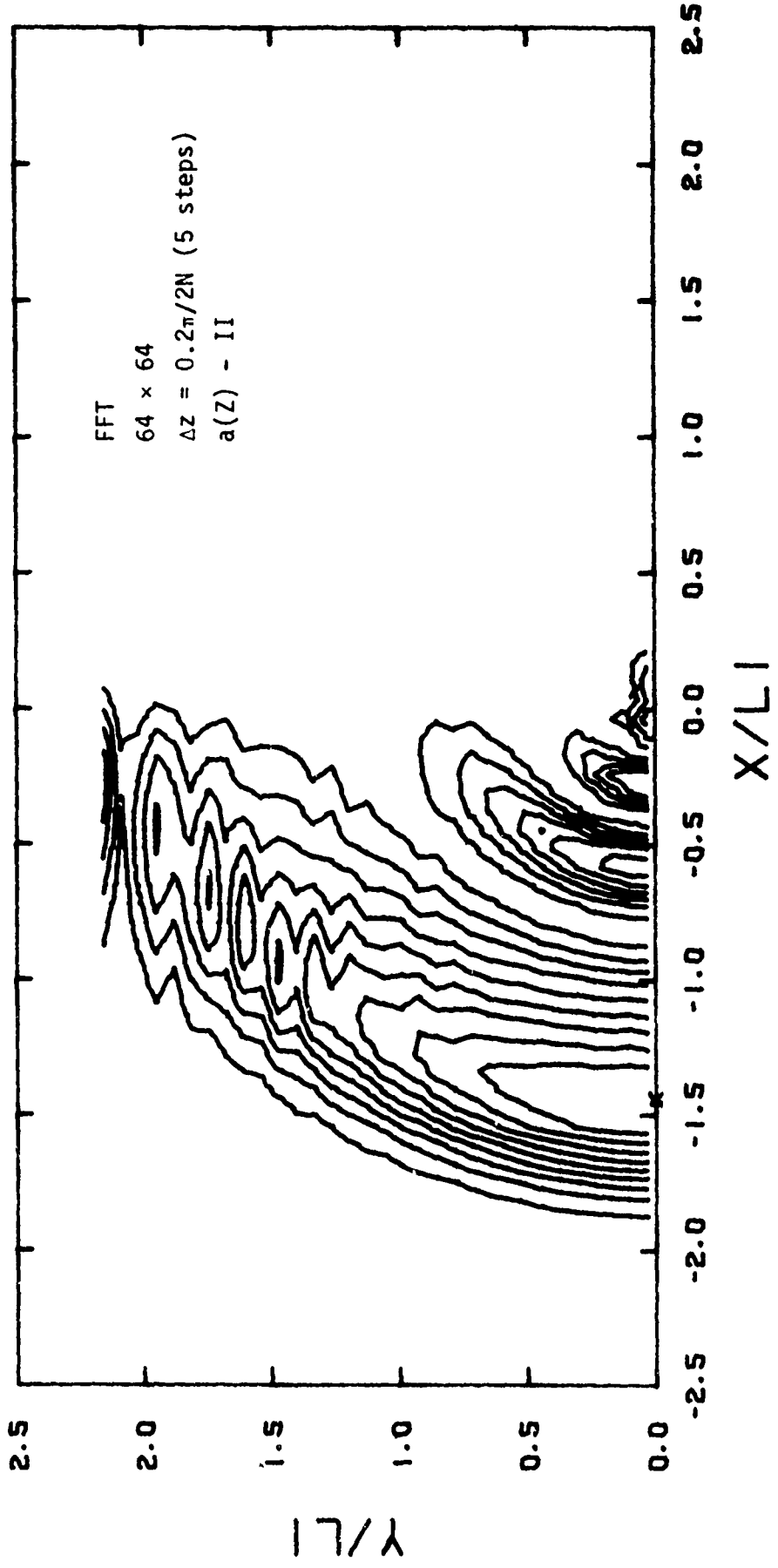
RUN NO. 723      ALPHA • 0.4480  
 Z/LE • 1.00      BETA • 8.2618  
 MAX. FLUX • 0.84      GAMMA • 44.0375



## ISO-IRRADIANCE CONTOURS

Figure 13. FFT Method - Excellent Solution with Coarser x,y Grid and No Nyquist Criterion (10 z Steps)

RUN NO. 723      ALPHA = 0.4480  
 Z/L2 = 1.00      BETA = 8.2618  
 MAX. FLUX = 0.60      GAMMA = 44.0375



## ISO-IRRADIANCE CONTOURS

Figure 14. FFT Method - Acceptable Solution with Coarser x,y Grid and No Nyquist Criterion (5 z Steps)

criterion is needed to sample the oscillations of the high frequencies. A similar behavior would be expected for the FFT method using (5-2) when  $\Delta z$  is relaxed. The difficulty does not occur using (5-10), since the oscillations are followed "exactly" for each frequency within the step. This does not imply that the solution itself is exact, since the phase transformations done at each step are obviously approximate.

## IX. CONCLUSIONS

The numerical solution of the laser propagation problem can be greatly enhanced by mathematical transformations that are applied concurrently. Transformations previously used can be generalized to remove phase oscillations arising from the focusing optics and still permit beams blooming well beyond a one times diffraction limited coordinate system. The FFT and IGS approaches to the solution of the propagation problem are found to differ most importantly in the fact that a step-size criterion similar to the Nyquist criterion is needed for IGS and can be relaxed for certain formulations of the FFT. Additionally, the FFT method yields greater accuracy than IGS for the same choice of gridding. While single steps of IGS are about 15 percent more efficient than FFT, the above factors led to a factor of 10 in computing efficiency for FFT for one sample problem, while for another problem the computing costs were about equal. Overall, the FFT method seems to be several times more efficient than the IGS method. Propagation programs based on the FFT method are easier to implement because of the general availability of FFT subroutines. This latter advantage is eliminated, however, when an IGS one-step subroutine is available. See Appendix B. The IGS method requires the storage of two complex arrays while FFT requires one. This is a significant saving of core storage for those problems that do not permit symmetry.

## ACKNOWLEDGMENTS

The author gratefully acknowledges consultation on this problem with Dr. P. Livingston, Naval Research Laboratory, Washington, DC. Dr. Livingston introduced the basic concepts of the model to the author and collaborated on obtaining one of the early numerical solutions (an explicit solution - 1971). Interest in the Fast Fourier Transform method arose from collaboration at the US Army Missile Command with Dr. J. Wallace and Dr. J. Lilly on the ARPA proposal, Reference 19. The author also gratefully acknowledges stimulating discussions and encouragement from his colleague, Dr. E. C. Alcaraz.



## REFERENCES

1. J. Wallace and M. Camac, "Effects of Absorption at 10.6  $\mu$  on Laser-Beam Transmission," *J. Opt. Soc. Am.*, Vol. 60, No. 2, 1970, pp. 1587-1594.
2. J. Wallace, "Effects of Nonlinear Refraction at 10.6  $\mu\text{m}$  on the Far-Field Irradiance Distribution," *J. Opt. Soc. Am.*, Vol. 62, No. 3, March 1972, pp. 373-378.
3. A. H. Aitken, J. N. Hayes, and P. B. Ulrich, "Propagation of High-Energy 10.6 Micron Laser Beams Through the Atmosphere," Naval Research Laboratory Report 7293, May 1971.
4. J. N. Hayes, P. B. Ulrich, and A. H. Aitken, "Effects of the Atmosphere on the Propagation of 10.6  $\mu$  Laser Beams," *Applied Optics*, Vol. 11, No. 2, 1972, pp. 257-260.
5. C. B. Hogge, "Thermo-Optical Effects of High-Energy Laser Beams," Air Force Weapons Laboratory Technical Report AFWL-TR-72-184, December 1972.
6. L. R. Bissonnette, "Thermally Induced Nonlinear Propagation of a Laser Beam in an Absorbing Fluid Medium," *Applied Optics*, Vol. 12, No. 4, April 1973, pp. 719-728.
7. P. M. Livingston, "Thermally Induced Modifications of a High-Power CW Laser Beam," *Applied Optics*, Vol. 10, No. 2, February 1971, pp. 426-436.
8. F. G. Gebhardt and D. C. Smith, "Investigation of Self-Induced Thermal Effects of CO<sub>2</sub> Laser Radiation Propagation in Absorbing Gases," United Aircraft Research Laboratories Annual Report K921004-4, April 1971.
9. J. Herrmann and L. C. Bradley, "Numerical Calculation of Light Propagation," Lincoln Laboratory, MIT, LTP-10, July 1971. In internal Lincoln Laboratory notes, the above authors describe how the IGS technique has been modified to account for beam blooming beyond a 1 times diffraction limited coordinate system. Reference to the Lincoln Laboratory method in this report does not reflect this modification.
10. F. G. Gebhardt and D. C. Smith, "Effects of Diffraction of the Self-Induced Thermal Distortion of a Laser Beam in a Crosswind," *Applied Optics*, Vol. 11, No. 2, 1972, pp. 244-248.
11. P. J. Lynch and D. L. Bullock, "An Integral Formulation of Propagation Through Inhomogeneous Media," TRW Report 99994-6215-RU-00, Redondo Beach, California, December 1972.

12. A. J. Glass, "The Method of Trajectories," Private Communication, Lawrence Livermore Laboratory.
13. P. B. Ulrich, "A Numerical Calculation of Thermal Blooming of Pulsed, Focused Laser Beams," Naval Research Laboratory Report No. 7382, December 1971.
14. P. B. Ulrich and J. Wallace, "Propagation Characteristics of Collimated, Pulsed Laser Beams Through an Absorbing Atmosphere," *J. Opt. Soc. Am.*, Vol. 63, No. 1, 1973, pp. 8-12.
15. J. Davis, K. Vogelsang, and T. Bleakney, Private Communication, Hughes Aircraft Company, Culver City, California.
16. H. B. Rosenstock, J. H. Hancock, and R. E. McGill, "Self-Defocusing of Light Propagating Through a Moving Gas," Naval Research Laboratory Memorandum Report No. 2289, July 1971.
17. W. P. Brown, "High-Energy Laser Propagation," Hughes Research Laboratories - Malibu, Midterm Technical Report, Contract N00014-73-C-0460, October 1973.
18. H. F. Harmuth, "On the Solution of the Schroedinger and the Klein-Gordon Equations by Digital Computer," *J. Math. Phys.*, Vol. 36, 1957, p. 269. This reference, while not concerned with propagation, does treat a mathematical problem of similar structure.
19. J. Wallace, "Proposal for a Study of Nonlinear Refractive Effects Associated with Stagnation Zones, Transonic-Supersonic Slewing, and Focal Spot Movement," ARPA Proposal from Far Field, Inc., Sudbury, Massachusetts, May 1973.
20. G. H. Canavan and D. E. Phelps, "Use of Fast Fourier Transforms in GDL Power Extraction Calculations," *Laser Digest*, AFWL-TR-73-131, p. 22, Air Force Weapons Laboratory, Kirtland Air Force Base, New Mexico, June 1973.
21. D. E. Phelps and G. H. Canavan, "Laser Propagation Using Fast Fourier Transforms," *Laser Digest*, AFWL-TR-73-273, p. 27, Air Force Weapons Laboratory, Kirtland Air Force Base, New Mexico, December 1973.
22. J. Wallace and J. Lilly, "Thermal Blooming for Repetitively Pulsed Lasers," US Army Missile Command Report to be Published.
23. A. Wood, M. Camac, and E. Gerry, "Effects of 10.6 Micron Laser-Induced Air Chemistry on the Atmospheric Refractive Index," *Applied Optics*, Vol. 10, August 1971, pp. 1877-1884.

24. J. Douglas and T. Dupont, "Alternating Direction Galerkin Methods on a Rectangle," in *Proceedings of the 2nd Symposium on the Numerical Solution of Partial Differential Equations*, B. Hubbard, ed., Academic Press, 1971, p. 133.
25. R. C. LeBail, "Use of Fast Fourier Transforms for Solving Partial Differential Equations in Physics," *J. Computational Physics*, Vol. 9, 1972, pp. 440-465.
26. R. W. Hockney, "A Fast Direct Solution of Poisson's Equation Using Fourier Analysis," *JACM*, Vol. 12, No. 1, January 1965, pp. 95-113.
27. J. Gazdag, "Numerical Convective Schemes Based on Accurate Computation of Space Derivatives," *Computational Physics*, Vol. 13, 1973, pp. 100-113.
28. N. M. Brenner, "Three Fortran Programs That Perform the Cooley-Tukey Fourier Transform," MIT Lincoln Laboratory Technical Note 1967-2, September 1967.
29. G. W. Hartwig, Jr., "CONTUR-A FORTRAN IV Subroutine for the Plotting of Contour Lines," BRL Memorandum Report No. 2282, March 1973.  
(AD # 760437)

## APPENDIX A

### USE OF FAST FOURIER TRANSFORM SUBROUTINES

The operation performed by a so-called FFT subroutine is the very rapid computation of the complex array

$$C_j = J^{-1} \sum_{\ell=1}^J D_{\ell} \exp[\nu i 2\pi (\ell - 1)(j - 1)/J] \quad (\text{A-1})$$

where the  $C_j$ ,  $j = 1, 2, \dots, J$ , are usually stored over the complex array  $D_{\ell}$ . For  $\nu = -1$ , this corresponds to the forward finite Fourier transform over discrete data. This is equivalent to obtaining the amplitudes of the  $J$  Fourier harmonics for approximating  $D$ . The approximation for  $D$  is then given by

$$D(x) = \sum_{j=1}^J C_j \exp[\nu i p_j x] \quad (\text{A-2})$$

where  $p_j$  is given by Equation (5-12) of the report and  $\nu = 1$ . If  $x$  is replaced by the discrete values over which  $D_{\ell}$  was defined, it can be shown that

$$\begin{aligned} D_{\ell} = D(x_{\ell}) &= \sum_{j=1}^J C_j \exp[\nu i p_j (\ell - 1)\Delta x] \\ &= \sum_{j=1}^J C_j \exp[\nu i 2\pi (j - 1)(\ell - 1)/J]. \end{aligned} \quad (\text{A-3})$$

The implication of this identity is that the sums (A-1) and A-3) can be performed by one algorithm with the appropriate change of  $\nu$ , as is done by the various available FFT routines. The possible pitfall in the propagation problem is that, in performing the integration of the wave function as approximated by the Fourier series, we must use the first sum in (A-3) rather than the second. Use of the convention standardized by the computer routines can obscure the fact that the second sum of (A-3) is a completely erroneous representation of the Fourier series at all points in  $x$  except the discrete points. The difficulty is avoided by observing that all operations involving  $x$  at other than the discrete points must treat the series as having the negative frequencies "folded" as given by Equation (5-12). These considerations affect only Equation (5-10) of the algorithm. Equations (5-11) and (5-14) involve situations where the sums of (A-3) are interchangeable.

The nature of the original Cooley-Tukey FFT algorithm and its many variants is such that the operation is far more efficient for arrays of length  $2^K$ . The computer code was designed to work with arrays of size  $64 \times 64$  to take advantage of this economy.



```

675 CALL GK(GKR,GKI,ID,I,J,DZOH2,B1RB,B1IB)
TOR=GKR-AIR*FKR(K-1)+AII*FKI(K-1)
TOI=GKI-AIR*FKI(K-1)-AII*FKR(K-1)
FKR(K)=TOR*PSIR(K)-TOI*PSII(K)
600 FKI(K)=TOR*PSII(K)+TOI*PSIR(K)
EKR(KMAX)=.0
EKI(KMAX)=.0
UKR=.0
UKI=.0
CO 1000 KK=1,KMAX
K=KMAX+1-KK
UKR=EKR(K)*UKRO-EKI(K)*UKIO+FKR(K)
UKI=EKR(K)*UKIO+EKI(K)*UKRO+FKI(K)
650 GOTD(600,700),ID
CHR(K,J)=UKR
CHI(K,J)=UKI
GOTO 800
700 CR(I,K)=UKR
CI(I,K)=UKI
800 CONTINUE
UKR=UKR
UKI=UKI
CONTINUE
IF(ID.EQ.1)GOTO 100
RETURN
END

```

SUBROUTINE GK(GKR,GKI,ID,I,J,DZOH2,B1RB,B1IB)

COMMON(USE MAIN)

SUBROUTINE EVALUATES GJ AND GK, EQS. (4-17) AND (4-27) OF  
 REP RT AS NEEDED BY ADVANC FOR IGS

```

AIR=1.
AII=1.*DZOH2
BIR=4.
BII=-3.*DZOH2
CIR=1.
CII=1.5*DZOH2
GOTD(100,200),ID
100 IF(I.EQ.1)ULR=.0
IF(I.NE.1)ULR=DR(I-1,J)
IF(I.EQ.1)ULI=.0
IF(I.NE.1)ULI=DI(I-1,J)
UCR=DR(I,J)
UCI=DI(I,J)
IF(I.EQ.IXM)URR=.0
IF(I.NE.IXM)URR=DR(I+1,J)
IF(I.EQ.IXM)URI=.0
IF(I.NE.IXM)URI=DI(I+1,J)
BR=BIR
BI=BII
IF(I.EQ.1.OR.I.EQ.IXM)BR=B1RB
IF(I.EQ.1.OR.I.EQ.IXM)BI=-B1IB
GOTO 300
200 IF(J.EQ.1)ULR=DHR(I,J+1)
IF(J.EQ.1)ULI=DHI(I,J+1)
IF(J.NE.1)ULR=DHR(I,J-1)
IF(J.NE.1)ULI=DHI(I,J-1)
UCR=DHR(I,J)
UCI=DHI(I,J)
IF(J.EQ.JYM)URR=.0
IF(J.NE.JYM)URR=DHR(I,J+1)
IF(J.EQ.JYM)URI=.0
IF(J.NE.JYM)URI=DHI(I,J+1)
BR=BIR
BI=BII
IF(J.EQ.JYM)BR=B1RB
IF(J.EQ.JYM)BI=-B1IB
300 CONTINUE
GKR=AIR*ULR-AII*ULI+BR*UCR-BI*UCI+CIR*URR-CII*URI
GKI=AII*ULR+AIR*ULI+BI*UCR+BR*UCI+CII*URR+CIR*URI
RETURN
END

```

## 11. LISTING OF FORTRAN IV SUBROUTINE FOR ONE STEP FFT ADVANCE

```

SUBROUTINE ADVANC(DRI,PV2,IXM,JYM,DZ02,ZOLD)
DIMENSION DRI(2,IXM,JYM),NN(2),PV2(IXM),WORK(130)
DIMENSION XIA(64),XRA(64)
REAL PART OF D IS STORED IN DRI(1,I,J)
IMAGINARY PART OF D IS STORED IN DRI(2,I,J)
PV2 CONTAINS THE SQUARE OF THE FREQUENCIES AS
DEFINED IN EQ.(5-12). THE ASSUMPTION IS THAT
J(IN REPORT)=IXM AND K(IN REPORT)=JYM, IXM=JYM,
DX=DY, HENCE P DEFINED BY EQ.(5-12) EQUALS
Q DEFINED BY EQ.(5-13).
DZ02=.5*DZ
ZOLD=VALUE OF Z AT BEGINNING OF STEP-THE ONLY
USE OF THIS ARGUMENT IS TO DETERMINE FIRST CALL
FROM SUBSEQUENT CALLS
FOURT-BRENNERS FFT SUBROUTINE-REF. 28
NN(1)=IXM
NN(2)=JYM
CALL FOURT(DRI,NN,2,-1,1,WORK)
CHECK FOR SKIPPING OF EVALUATION OF COMPLEX ARRAY
IF(ZOLD.EQ..0)GOTO 25
IF(ABS(DZ02-DZ02).GT..1E-7)GOTO 25
GOT 75
25 DO 50 I=1,IXM
PHI=-DZ/2*PV2(I)
XRA(I)=COS(PHI)
50 XIA(I)=SIN(PHI)
75 CONTINUE
DO 100 I=1,IXM
DO 100 J=1,JYM
DEN=FLOAT(NN(1)*NN(2))
YR=DRI(1,I,J)/DEN
YI=DRI(2,I,J)/DEN
XR=XRA(I)*XRA(J)-XIA(I)*XIA(J)
XI=XRA(I)*XIA(J)+XRA(J)*XIA(I)
DRI(1,I,J)=XR*YR-XI*YI
DRI(2,I,J)=XI*YR+XR*YI
100 CONTINUE
CALL FOURT(DRI,NN,2,1,1,WORK)
DZ02=DZ/2
RETURN
END

```

## LIST OF SYMBOLS

B	Transformed complex wave function
$c_p$	Specific heat of propagation medium at constant pressure
D	Transformed complex wave function
$F(\xi, \eta)$	Spatial distribution of beam amplitude at aperture
k	Wave number ( $= 2\pi/\lambda$ )
L	Characteristic length in propagation direction ( $= R$ , focused beams; $= kr^2$ , collimated beams)
n	Index of refraction after laser heating (function of $\xi$ , $\eta$ , and $\zeta$ )
$n_0$	Index of refraction under ambient conditions (assumed constant)
P	Total beam power
r	Characteristic length in $\xi$ - $\eta$ plane; $e^{-1}$ folding length for a Gaussian beam
R	Focal distance for focused beam
T	Atmospheric temperature after laser heating (function of $\xi$ , $\eta$ , and $\zeta$ )
$T_0$	Ambient atmospheric temperature
U	Dimensionless complex wave function ( $= W/W_0$ )
V	Wind speed (assumed to be in the positive $\xi$ direction and may be $\zeta$ -dependent)
W	Complex wave function
$W_0$	Normalizing factor [ $= (P/\pi r^2)^{1/2}$ ]
x, y	Adaptive coordinates in transverse plane [ $= X/a(Z)$ , $Y/a(Z)$ ]
X, Y	Dimensionless spatial coordinates in transverse plane ( $= \xi/r$ , $\eta/r$ )
Z	Dimensionless coordinate in propagation direction ( $= \zeta/L$ )
z	Transformed coordinate in propagation direction [see Eq. (3-3)]
$\alpha_1$	Absorption coefficient
$\alpha$	Dimensionless absorption coefficient ( $= \alpha_1 L$ )
$\beta$	Dimensionless parameter ( $= kr^2/L$ ), equal to the Fresnel number for focused beams or unity for collimated beams
$\gamma$	Dimensionless thermal blooming distortion parameter [ $= (n_0^2 - 1)P/(T_0 \rho_0 c_p V \lambda r)$ ]; in the atmosphere $\gamma$ may be $\zeta$ -dependent.
$\zeta$	Spatial coordinate in propagation direction
$\xi, \eta$	Spatial coordinates in transverse plane
$\lambda$	Laser wavelength



- $\mu$  Dimensionless quantity  $[= \frac{1}{2} kL(n^2 - n_0^2)]$
- $\rho$  Atmospheric density after laser heating (function of  $\xi, \eta, \zeta$ )
- $\rho_0$  Ambient atmospheric density
- $\phi$  Spatial distribution of beam phase at aperture
- $\Omega$  Angular slewing velocity
- $\omega$  Dimensionless slewing velocity  $(= \Omega L/V)$